

ULTRASHORT LASER PULSES

Carlo Antoncini
Department of Physics
University of Reading
Whiteknights, Reading, RG6 6AF, UK

Abstract: *Ultrashort laser pulses are considered to be those whose pulse duration is less than a few picoseconds (10^{-12} s) long. Recent research has led to techniques such as Kerr-lens mode locking to enable pulse duration down to around 5 femtoseconds (10^{-15} s) and chirped pulse amplification giving pulses peak powers of several terawatts. In very recent years research has driven towards the attosecond regime (10^{-18} s), allowing for the possibility to probe such phenomena as the motion of electrons, by utilising the progress in ultrashort laser pulses. The best commercially available lasers operate mode-locked with titanium sapphire as the gain medium and the Ultrafast Laser Laboratory at the University of Reading is an excellent example. This article reviews the generation and measurement of ultrashort pulses and discusses their future.*

Introduction

Einstein used the quantisation of electromagnetic energy, as Planck had done five years earlier in his work on black-body radiation, to explain the photoelectric effect in 1905. After Bohr had published his model of the atom in 1913 giving orbiting electrons fixed energy levels, Einstein was able to conclude in 1917 that an interaction existed between light and matter called stimulated emission that would amplify light.

‘A solution looking for a problem’⁽¹⁾ is how many scientists described the first working laser, set up by Theodore Maiman in 1960. The gain medium used by Maiman was ruby ($\text{Cr}^{3+}:\text{Al}_2\text{O}_3$), which is sapphire (Al_2O_3) with a small number of aluminium ions (Al^{3+}) replaced by chromium ions (Cr^{3+}).

A laser can be described as an optical source that emits a coherent beam of photons at an exact wavelength or frequencies. For example, a 0.05% concentration of Cr^{3+} (pink ruby – the colour is due to absorption in the green and violet parts of the spectrum) gives a laser wavelength of 694.3 nm where a 0.5% concentration (red ruby) gives either 700.9 nm or 704.1 nm wavelengths. In stark contrast other common light sources emit incoherent light in all directions, normally over a wide range of wavelengths or frequencies.

All lasers have some very important components in common. With reference to Figure 1 these are the laser’s gain medium (1), an energy source to pump the laser medium (2), a highly reflective mirror (3) and a partially reflective mirror (4). The highly reflective mirror and the partially reflective mirror, or output coupler, are aligned so as to cause most of the light to oscillate between them through the gain medium. With each trip the light

undergoes further amplification. The partially reflective mirror reflects most of the light incident on it but allows a small percentage to be transmitted through, forming the laser output (5).

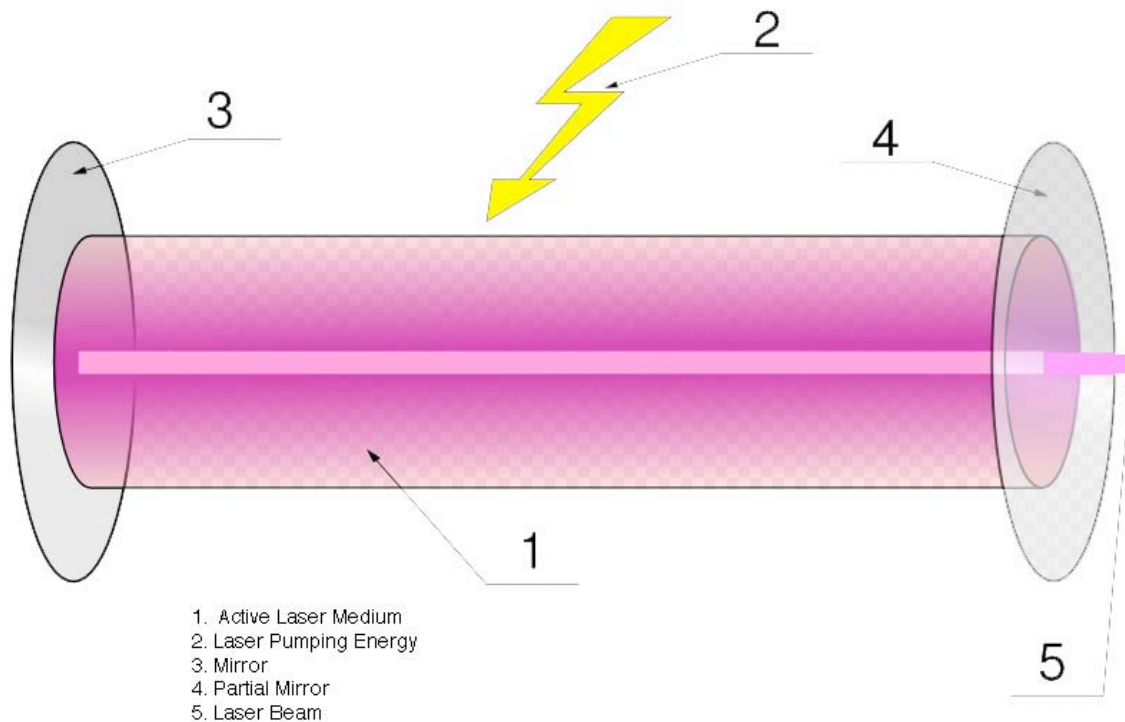


Figure 1⁽²⁾ – A schematic of a laser set-up.

In most materials light is absorbed, though in some the light is amplified. The only real difference is the state the atoms are in before they interact with light (see Figure 2). The energy for pumping the laser (Figure 1.2) needs to be resonant with the system to raise atoms to an excited state and then to stimulate them into emitting photons. For the ruby laser a flash lamp was used, though typically today a continuous wave (CW) laser is used to supply light at the correct wavelength for absorption and emission in the gain medium.

Einstein concluded that there are three interactions between matter and light, which are shown in Figure 2.

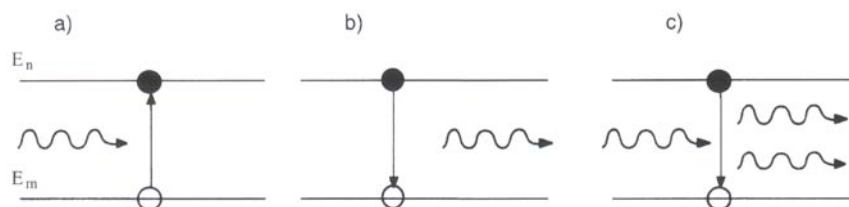


Figure 2⁽³⁾ – The interactions between light and matter.

a) *Absorption* – A photon, with energy $\hbar\omega$, from the radiation field transfers its energy to an electron as potential energy when it moves from E_m to E_n , raising the atom's energy and putting it in an excited state.

b) *Spontaneous Emission* – When an electron in an excited state E_n drops to a lower state E_m via decay there is a loss of potential energy in the atom. This is released as a photon and the photon's energy is equal to $E_n - E_m = \hbar\omega$. The released photon's phase, direction and polarisation are all random.

c) *Stimulated Emission* – When an electromagnetic field is present around an atom, a photon with energy $\hbar\omega$ can stimulate the emission of a twin photon from an excited atom. This twin photon is emitted with identical energy, direction, phase and polarisation as the inducing photon, thus amplifying the energy.

Each stimulated emission, or spontaneous emission, event returns an atom to its ground state, reducing the number of atoms in the medium available for further amplification. For laser action to occur more atoms need to be in an excited state than in the ground state and when this is achieved it is known as a population inversion. If the pump power is not strong enough to produce a gain that will overcome cavity losses (spontaneous emission) to produce a population inversion then the laser can only emit very low powers. The transition at where the pump power creates a gain strong enough for population inversion is appropriately known as the laser threshold.

The physics of producing laser light is something that is very well understood today and there are a large number of resources^(4,5,6,7,8) that explain the subject at a variety of academic levels.

Ultrafast Laser Laboratory

The Ultrafast Laser Laboratory (ULL) at the University of Reading Physics department is a fairly typical example of one of the most advanced, commercially available lasers of today. It enables a broad range of study of laser interactions with matter and fundamental optics⁽⁹⁾.

The most recent advances in the field of ultrashort pulse generation have been around the development of titanium-doped aluminium oxide (Ti:Sapphire – $\text{Ti}^{3+}:\text{Al}_2\text{O}_3$) as a gain medium. Ti:Sapphire was introduced in 1986⁽¹⁰⁾ and is the most favoured gain medium, producing ultrashort pulses with good beam quality and high output power.

As the Cr^{3+} ion did in ruby, the Ti^{3+} ion replaces the Al^{3+} ion in the sapphire structure by up to a few percent thanks specifically to progress in crystal growth. The ionic radius of the titanium ion is 26% larger than the aluminium one it replaces, inducing a strong local distortion in the titanium ion, which then creates a strong local electric field. This means the absorption band is abnormally wide in the blue-green part of the spectrum. Under influence from the generated local electric field the absorption at these visible wavelengths excites electrons from a 2T_g ground state to a 2E_g excited level, which then splits into two sublevels 50 nm apart.

The vibrational modes of the sapphire matrix are strongly coupled with the ground and excited states of the Ti^{3+} ion, which induces strong homogenous broadening. Further important points are that sapphire has excellent thermal conductivity, which relieves thermal effects at high powers and intensities. The Ti^{3+} ion has an extremely large gain bandwidth, allowing for generation of ultrashort pulses and wide wavelength tunability, with maximum gain and laser efficiency gained at 800 nm. The tuning range is from 650 nm to 1100 nm⁽¹¹⁾.

Figure 3 shows the main components for creating and manipulating the ultrashort pulses at the ULL.

1. Coherent Verdi V5⁽¹²⁾ is the optical pump for the oscillator.
2. Coherent Mira Seed⁽¹³⁾ femtosecond mode-locked Ti:Sapphire laser.
3. Coherent Evolution 30⁽¹⁴⁾ pump laser for the regenerative amplifier.
4. Coherent Legend USP-High Energy⁽¹⁵⁾ femtosecond regenerative amplifier.

Figure 31a is the pulse measurement device SPIDER (20 fs to 80 fs model) from APE⁽¹⁶⁾.

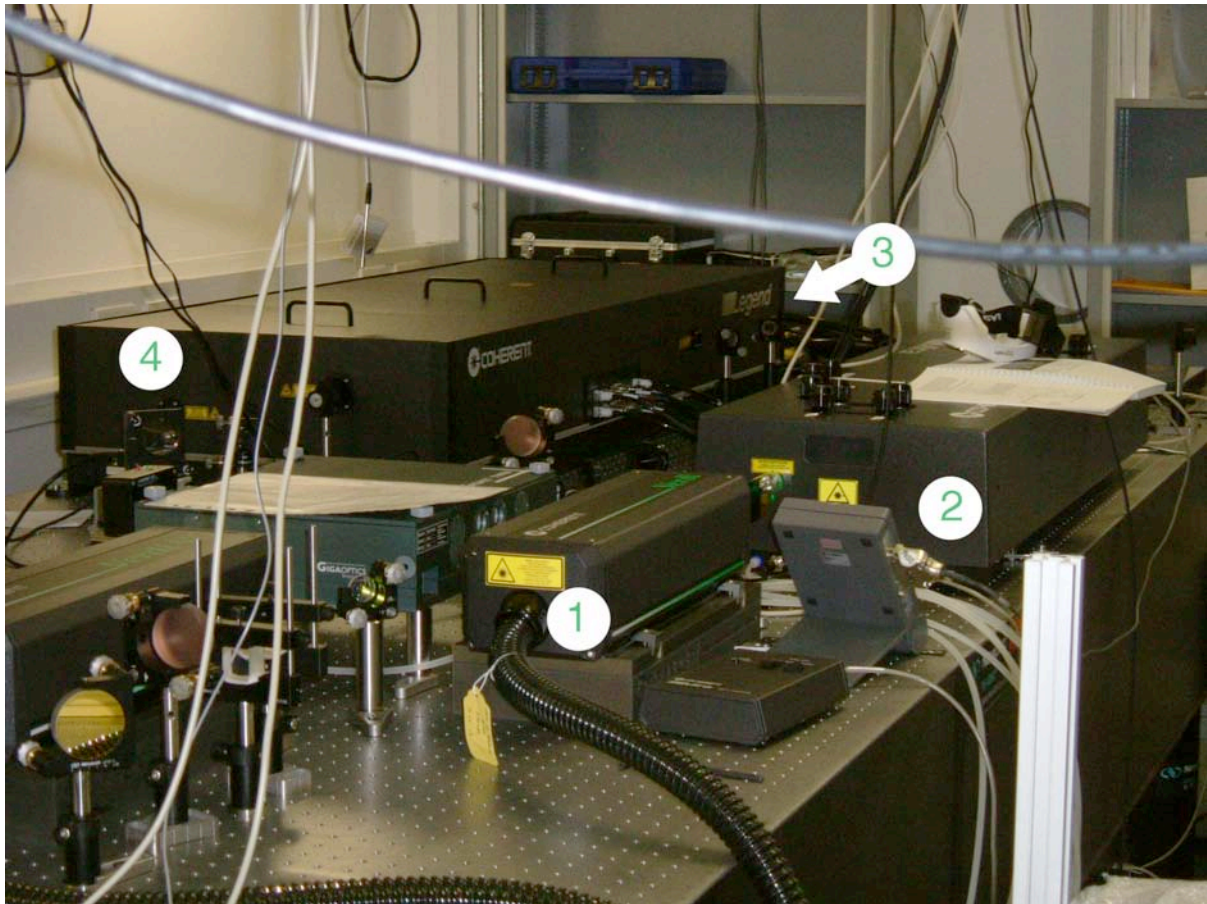


Figure 3 – The Ultrafast Laser Laboratory at the University of Reading, Department of Physics.

Ultrashort Pulses

Ultrashort pulses are generated using mode-locked lasers and are defined as having a pulse duration of a few tens of picoseconds at the very most. De Maria *et al*⁽¹⁷⁾ produced the first ultrashort pulses just six years after Maiman's first laser was demonstrated. In addition to ultrashort pulse duration, ultrashort pulses have a broad spectrum, a high peak intensity and can form pulse trains at a high repetition rate.

First it is important to acknowledge the relationship between spectral width and pulse duration when considering the generation of ultrashort pulses. The general time and frequency Fourier transforms of a pulse⁽¹⁸⁾ are,

$$\begin{aligned}\varepsilon(t) &= \frac{1}{2\pi} \int_{-\infty}^{+\infty} E(\omega) e^{-i\omega t} d\omega, \\ E(\omega) &= \int_{-\infty}^{+\infty} \varepsilon(t) e^{i\omega t} dt.\end{aligned}\tag{Equation 1}$$

The duration and spectral width of a pulse can then be calculated with standard statistical definitions,

$$\begin{aligned}\langle \Delta t \rangle &= \frac{\int_{-\infty}^{+\infty} t |\varepsilon(t)|^2 dt}{\int_{-\infty}^{+\infty} |\varepsilon(t)|^2 dt}, \\ \langle \Delta \omega^2 \rangle &= \frac{\int_{-\infty}^{+\infty} \omega^2 |E(\omega)|^2 d\omega}{\int_{-\infty}^{+\infty} |E(\omega)|^2 d\omega}.\end{aligned}\tag{Equation 2}$$

These quantities can then be related by the following inequality,

$$\Delta t \Delta \omega \geq \frac{1}{2}.\tag{Equation 3}$$

Equation 3 is the product of pulse duration and spectral bandwidth and is known as the time-bandwidth product. In principle this means that in order to generate a short pulse of light with a specific duration (Δt) a broad spectral bandwidth ($\Delta \omega$) is required. For example, if a pulse is to last a picosecond (10^{-12} s) then the spectral bandwidth must be at least 441 MHz ($\Delta \omega = 4.41 \times 10^{11}$ Hz). When equality to $\frac{1}{2}$ is reached in Equation 3 the pulse is called a Fourier transform-limited pulse. The variation in phase of such a pulse is beautifully uniform and so has linear time dependence; the instantaneous frequency is time independent.

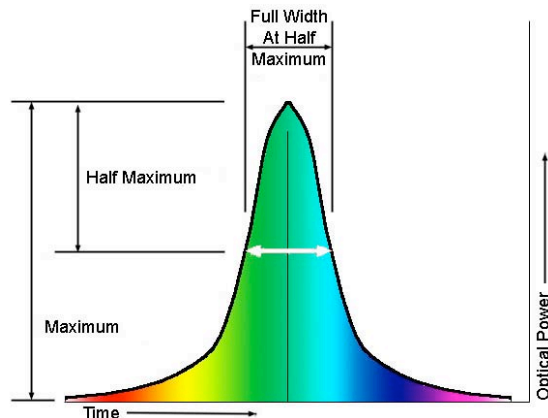


Figure 4⁽¹⁹⁾ – The measurement of 'full width at half maximum' of a pulse to find its duration.

This can define pulse duration, though the more commonly used definition is based on the full-width at half-maximum (FWHM) principle of optical power against time, as in Figure 4, because experimentally it is easier to measure. Equation 3 then becomes

$$\Delta \nu \Delta t \geq K.\tag{Equation 4}$$

$\Delta\nu$ is the frequency at full-width half-maximum and Δt is the duration at half maximum. The value of K from Table I depends upon the symmetrical shape of the pulse.

Shape	K
Gaussian function	0.441
Exponential function	0.140
Hyperbolic secant	0.315
Rectangle	0.892
Cardinal sine	0.336
Lorentzian function	0.142

Table I⁽²⁰⁾ – Various values for K depending on the pulse shape.

The ULL - Optical Pump 1

An optical pump (Figure 3.1) at the correct wavelength is required to provide energy to the gain medium in the oscillator. Ti:Sapphire requires a pump in the blue-green region of the spectrum and although there is a wide range of pump wavelengths available there are no laser diodes powerful enough in this spectral region. Several watts of pump power are needed because the upper-state lifetime of Ti:Sapphire is very short at 3.2 μs and the saturation power, the incident optical power required to achieve significant saturation of an absorber⁽²¹⁾, is very high. Originally Ti:Sapphire lasers were pumped using argon-ion lasers at 514 nm, which were powerful but bulky, inefficient and expensive to run.

The ULL uses a CW solid-state, frequency-doubled, neodymium-doped, yttrium orthovanadate (Nd:YVO₄) laser to provide 5W of power to the oscillator at 532 nm. The laser is frequency-doubled because its lasing wavelengths are 914 nm, 1064 nm and 1342 nm. Taking $c = \lambda\nu$ (speed of light [c] = wavelength [λ] * frequency [ν]) into account it is clear that doubling the frequency will halve the wavelength, bringing the middle lasing wavelength (1064 nm) into the green part of the spectrum (532 nm).

Figure 5a is the Verdi V5 in CW operation and in Figure 5b the green laser output can be seen as it is partially scattered by dust particles in the air. The box to the right is the oscillator into which this pump beam is fed.

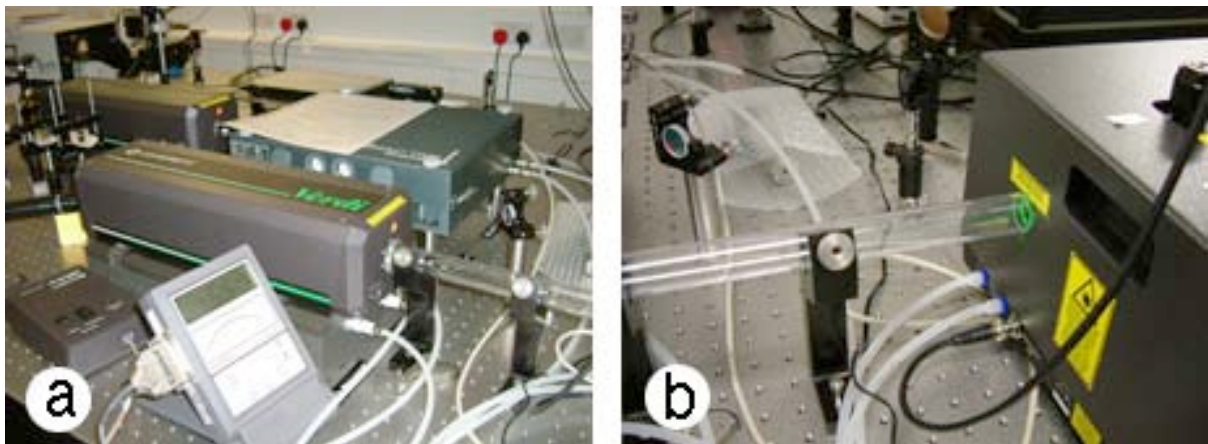


Figure 5 – Verdi V5 Nd:YVO₄ pump laser.

The ULL - Oscillator

The laser oscillator (Figure 3.2), or optical resonator, is an intricate device as Figure 19 indicates. The Mira Seed in the ULL is a femtosecond mode-locked Ti:Sapphire laser. In the most simplistic terms the oscillator allows a single short, pulse of light to bounce back and forth between its mirrors. With the modes locked in phase a pulse can be formed and each time the pulse reaches the output coupler, a partial mirror, a small percentage of is allowed to pass through to form the output of the laser.

The time between these pulses is equal to the time it takes for the pulse to do one round-trip of the cavity, as in Equation 9, and for the Mira Seed this takes approximately 13.2 ns⁽²²⁾. The number of pulses output per second can be calculated as time and frequency have an inverse relationship.

$$\text{Frequency} = \frac{1}{T} = \frac{1}{13.2 \times 10^{-9} \text{ s}} = 7.576 \times 10^7 \text{ Hz.} \quad \text{Equation 5}$$

This gives the pulse repetition rate of the Mira Seed to be 76 MHz. Only a single pulse forms each trip as excited atoms in the gain medium are returned back to the ground state so for a short while there are insufficient excited atoms to amplify a second pulse.

Longitudinal Modes

The existence of longitudinal modes is the most important characteristic of an optical resonator when using lasers as short pulse generators. Longitudinal modes, sometimes called axial modes, are known as a time-frequency property.

For laser oscillations to occur within a cavity a wave must be able to self-replicate after two reflections so that the electric fields constructively interfere and add up in phase. When an electromagnetic wave propagating between two parallel mirrors adds constructively with an electromagnetic wave propagating in the reverse direction an electromagnetic field is established. The mirrors have now formed a resonant cavity and the resulting waves are known as standing waves, much like those that develop on a plucked guitar string.

A standing wave can only exist if the distance between the parallel mirrors is a positive integer multiple of the half-wavelength of the light. All other frequencies of light consequently destructively interfere. The discrete sets of frequencies that are formed directly from these standing waves are then called the longitudinal modes of the cavity.

The condition for a standing wave, where λ is the wavelength of light and the length of the cavity is L , is

$$\frac{m\lambda}{2} = L. \quad \text{Equation 6}$$

The value of the positive integer m is known as the mode order and it can be quite large. For example a cavity length $L = 0.5 \text{ m}$ and $\lambda = 500 \text{ nm}$, m is about 2×10^6 , meaning there are many possible values of m for just a small change in wavelength, λ .

Using $\nu = c/\lambda$, Equation 6 can be written as

$$\nu = \frac{mc}{2L}. \quad \text{Equation 7}$$

The frequency separation $\Delta\nu$ between adjacent modes ($\Delta m = 1$) is also of importance and can be found using

$$\Delta\nu = \frac{c}{2L}. \quad \text{Equation 8}$$

The round-trip time of flight, T , in the cavity is very easily calculated using Equation 9,

$$T = \frac{2L}{c}. \quad \text{Equation 9}$$

For a fairly typical laser the cavity length $L = 1.5$ m, so the period $T = 10$ ns. This gives a characteristic frequency of $\nu = 100$ MHz⁽²³⁾. It's these numbers that control the repetition rate of the mode-locked laser and the period of the pulse train.

Although there are a large number of longitudinal modes (Equation 6) in the cavity, spaced from adjacent modes by Equation 8, they can only oscillate if there is gain at their specific frequency. Figure 6 shows schematically how not all of the frequencies are amplified and therefore do not all contribute to the laser output spectrum. The amplifying medium in the laser only amplifies over certain frequencies.

The gain medium, primarily determines the bandwidth over which the laser may operate. The bandwidth of a laser can be quoted in either frequency or wavelength as the two have an inverse relationship. Converting between nanometres and gigahertz depends on the central wavelength or frequency. To convert a small wavelength interval, $\Delta\lambda$, into a frequency interval, $\Delta\nu$, the following relation is needed

$$\Delta\nu = \frac{c}{\lambda^2} \Delta\lambda. \quad \text{Equation 10}$$

Analysis of Equation 10 shows that one nanometre is worth more than one gigahertz if the central wavelength, λ , is shorter (note that c is the speed of light). It is generally accepted that Ti:Sapphire has a bandwidth of around 128 THz, which corresponds to around a 300 nm wavelength range and could potentially support approximately 250,000 modes (for a 30 cm cavity)⁽²⁴⁾. Compared to a medium such as helium:neon (HeNe), which has 1.5 GHz bandwidth (a 0.002 nm wavelength range) and could support just 3 longitudinal modes (again a 30 cm cavity), it's clear why Ti:Sapphire is the saviour of the mode-locked laser.

Figure 6 also highlights the fact that it is both the bandwidth of the laser and the number of longitudinal modes allowed to oscillate, that are responsible for the laser's output spectrum.

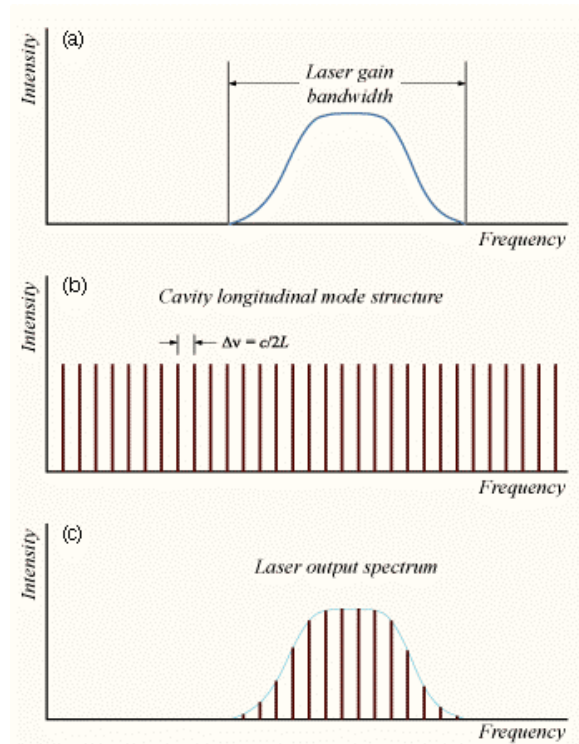


Figure 6⁽²⁵⁾ – A schematic of the longitudinal mode structure in a laser. (a) The laser’s gain medium will only amplify light over a certain range of frequencies. This refers to a laser’s gain bandwidth. (b) The longitudinal modes are equally spaced by Equation 8. (c) Only the modes whose corresponding frequencies fall into the laser’s gain bandwidth will be amplified.

Mode-Locking

Figure 7 shows how the time distribution of a laser output depends upon the phase relations between the modes. Figure 7a shows how the intensity varies from a single oscillating mode and Figure 7b is the resultant intensity of two modes in phase with each other. Figure 7c gives an idea of how eight modes with random phase relations to one another give a random distribution of intensity maxima, but let these eight modes oscillate with the same initial phase, Figure 7d, and a period repetition of a wave packet from the resultant constructive interference can be seen.

When a laser operates naturally it will oscillate simultaneously over all resonant frequencies of the cavity, as long as the unsaturated gain remains greater than the cavity losses. A mode-locked femtosecond laser requires a broadband gain medium, such as Ti:Sapphire, which can sustain over 100,000 longitudinal modes in a laser cavity⁽²⁶⁾. While operating in this free multi-mode regime there is usually strong competition between modes to be amplified by the stimulated emission of the same atoms in the gain medium. The fluctuations in the output intensity of the laser (Figure 7c) can be explained by this competition, which causes big fluctuations in the relative phases and amplitudes of the modes.

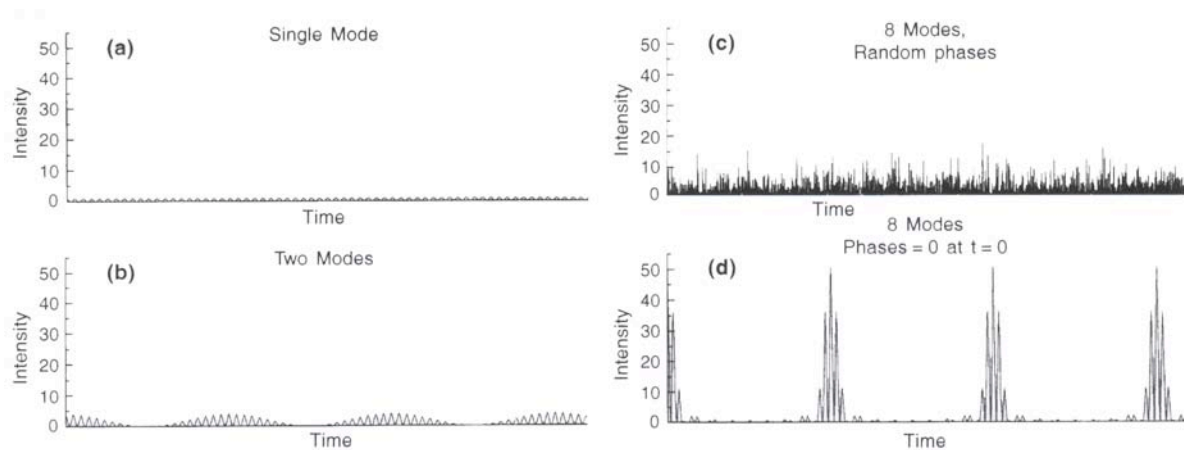


Figure 7⁽²⁷⁾ – The influence of the phase relation between oscillating modes on the output intensity of the oscillation. (a) is a single mode, (b) two modes in phase, (c) eight modes with random phases and (d) eight modes in phase.

The purpose of mode-locking is to organise the modes so that the relative phases are constant, which is equivalent through Fourier transformation to the output intensity of the laser consisting of a periodic series of pulses that are the result of a wave packet oscillating back and forth in the cavity.

Considering in the time domain, the competition inside a wave packet travelling back and forth in the cavity sees that the initially slightly stronger maxima will grow much stronger at the expense of the lesser maxima. Choosing the conditions correctly will see a single concentrated pulse oscillating containing all of the energy of the cavity. This is a mode-locked situation: in the time domain selecting a single intensity maximum is equivalent in the frequency domain to establishing a relation between the phases of the longitudinal modes.

Switching to the frequency domain, if a device in the cavity can modulate the modes at a frequency close to the frequency separation interval of the modes, $\Delta\nu$, then competition for gain in the gain medium results in a coupling between each mode and the sidebands from the modulation of the adjacent modes. The two main methods of mode-locking, active and passive, are formed from these two ideas.

Active Mode-Locking

Active mode-locking is a technique for generating ultrashort pulses by modulating the cavity losses or modulating the round-trip phase change. This is done with either an acousto-optic or electro-optic modulator, see Figure 8 for its position in the cavity. Ultrashort pulses are generated if the modulation is synchronised with the cavity round-trips.

Using an acousto-optic modulator is the most common method and when driven with an electrical signal a sinusoidal amplitude modulation (AM) of each longitudinal mode is induced. If the modulation frequency is driven close to the intermode frequency separation, $\Delta\nu$ (Equation 8), the two sidebands will be very close to the adjacent modes of a chosen mode. The sidebands and longitudinal modes will now compete against each other in the gain medium for maximum amplification. However, the most efficient use of the energy in the gain medium is for the longitudinal modes to lock their phases onto the sidebands, which

in turn causes a global phase-locking over the whole spectral distribution. Global phase-locking will yield a single oscillating pulse that contains all the energy of the cavity.

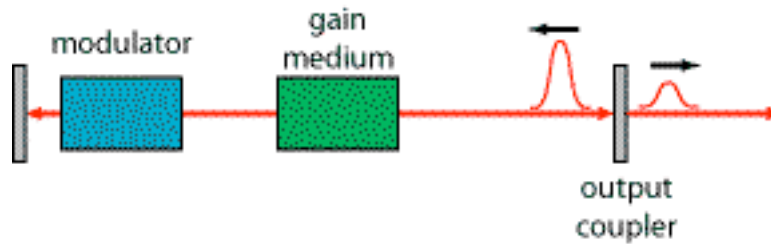


Figure 8⁽²⁸⁾ - The position of a modulator in an actively mode-locked laser set-up.

In the time domain the modulator can be thought of as a weak shutter. It attenuates the oscillating light when closed and lets it pass through when open. Figure 9 shows how a perfectly timed pulse can pass by the modulator at the exact moments where the losses are at a minimum. The wings of the pulse overlap the modulation signal slightly and so encounter a small amount of attenuation, which effectively shortens the pulse slightly on every round-trip. If the modulation rate is the same as the round-trip time, T (Equation 9), then just a single pulse will oscillate in the cavity. This shortening is finite and is typically limited to the picosecond range. An attenuation of just 1% is enough to mode-lock as the same part of the light is repeatedly attenuated as it propagates through the cavity.

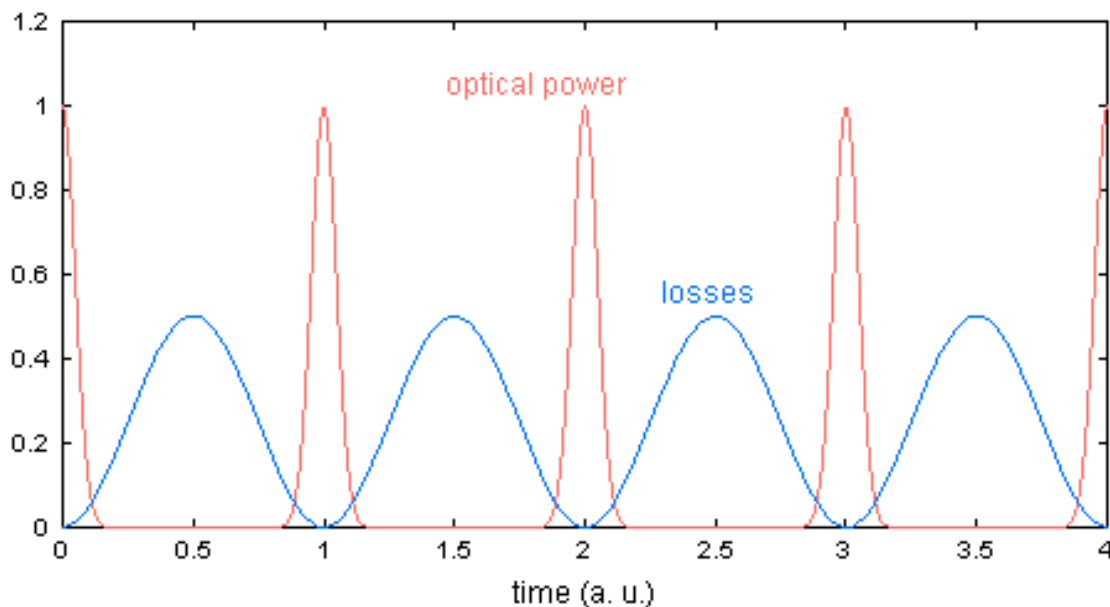


Figure 9⁽²⁹⁾ – The temporal evolution of optical power and losses due to active mode-locking.

Active mode-locking can also work by a periodic phase modulation using a modulator based on the electro-optic effect and this is called frequency modulation (FM) mode-locking. This device when driven with an electrical signal induces a small, sinusoidal varying frequency shift in the light that passes through it.

Again matching the frequency of the signal to the round-trip time will cause some of the light to be repeatedly up-shifted in frequency and some of it to be repeatedly down-shifted. Eventually this light will be shifted far enough to be outside of the laser gain

bandwidth. The only light left unaffected is that which passes through the modulator at the exact time when the induced frequency shift is at a minimum of zero and this leaves a narrow pulse of light oscillating. This method, however, leads to a chirped pulse – one whose instantaneous frequency changes with time.

Passive Mode-Locking

Passive mode-locking works by placing a saturable absorber inside the laser cavity, which does not need an external modulating signal to operate. This method introduces a self-amplitude modulation into the cavity and allows far shorter pulses than active mode-locking because a saturable absorber, when driven by already very short pulses, can modulate cavity losses far quicker than any electronic modulator.

A saturable absorber is an optical device, usually a semiconductor saturable absorber mirror (SESAM), with an intensity-dependent transmission property, meaning it will allow transmission of high intensity light and will absorb low intensity light. Dyes can also be used but they are very wavelength dependent and often exist in liquid form so have to be refreshed regularly or be free flowing. Additionally the concentration of these dyes has to be altered as the laser power changes. A SESAM normally consists of a Bragg mirror, which has alternating layers of two different optical materials with optical thickness corresponding to one quarter of the wavelength of light for which the mirror is designed. The reflectivity then varies with the intensity of light incident upon it. Figure 10 shows the position of a saturable absorber in a laser set-up.

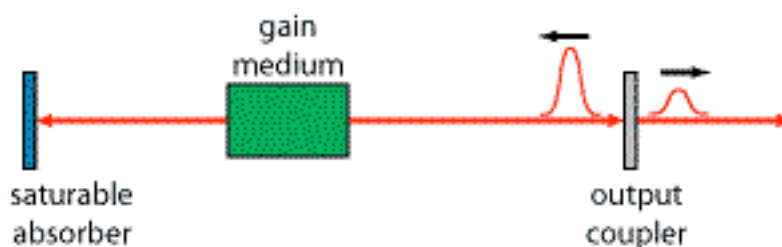


Figure 10⁽³⁰⁾ – Saturable absorber set-up in a passively mode-locked laser.

As a pulse begins to form it travels through the cavity encountering the gain medium and the saturable absorber. When the pulse reaches the saturable absorber the leading edge is strongly absorbed. The relaxation time of the absorber in a Ti:Sapphire laser is longer than the pulse duration, which means that the tail of the pulse will pass through the now saturated absorber without being attenuated.

Once the pulse reaches the gain medium the leading edge will be strongly amplified by the unsaturated gain, while the tail of the pulse will experience a much lesser amplification as the gain becomes saturated. After oscillating many times, the pulse will have a very strong maximum and be very narrow because the centre of the initial pulse is not affected by the absorber and is amplified by the gain medium, whereas the wings feel the opposite and are attenuated. Any other oscillating low intensity light experiences more loss than gain and subsequently dies out during further round-trips.

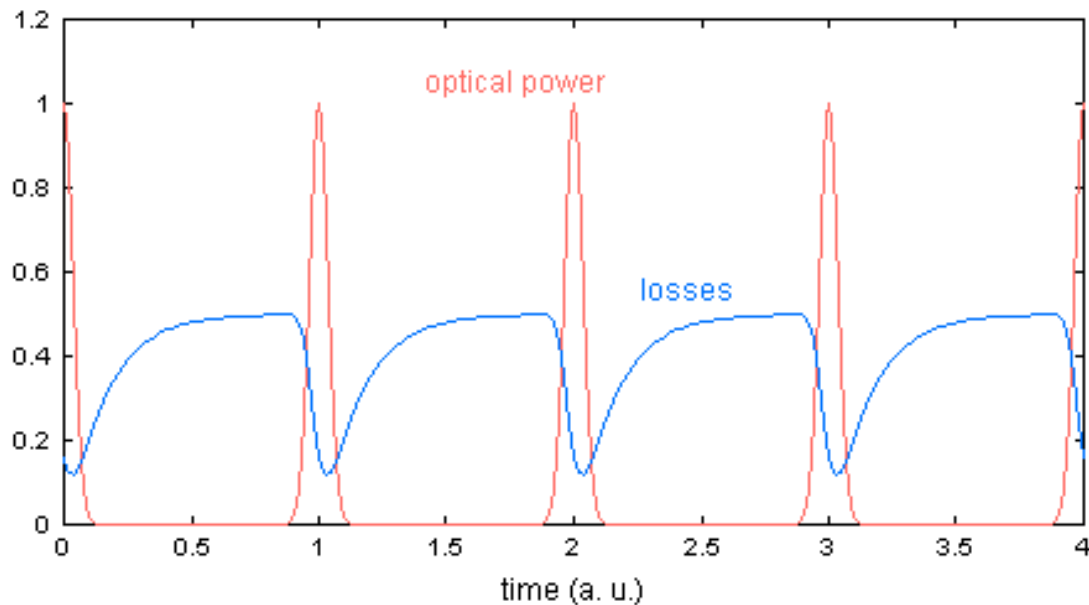


Figure 11⁽³¹⁾ – The temporal evolution of optical power and losses due to passive mode-locking with a slow saturable absorber. The ratio of pulse duration to pulse period is much smaller in reality.

All absorbers for ultrashort pulses are slow absorbers and have a recovery time larger than the pulse duration, as seen in Figure 11.

Kerr Lens Mode-Locking

Ti:Sapphire was discovered as gain medium with the bandwidth that could support femtosecond pulses in 1986⁽¹⁰⁾ and it was generally assumed that everything was known about mode-locked femtosecond lasers by the end of the 80s⁽³²⁾. However, 1990 saw two important discoveries. Ishida *et al*⁽³³⁾ produced stable 190 fs pulses using a passively mode-locked Ti:Sapphire laser with a saturable absorber. Then Sibbet *et al*⁽³⁴⁾ showed it was possible to produce 60 fs pulses from a Ti:Sapphire laser that appeared to have no saturable absorber at all. Sibbet's mode-locking approach was initially termed 'magic mode-locking' and a huge research effort was launched to understand these results. The phenomenon was soon understood and is now called Kerr lens mode-locking (KLM)⁽³⁵⁾. It also explained Ishida's result.

The optical Kerr effect is a nonlinear interaction of light in a medium with an instantaneous response. The Kerr effect can be described as a modification of the refractive index in response to an electric field. Scottish physicist John Kerr discovered the occurrence in 1875 and the effect can occur in glasses, crystals and gases, though certain materials display the effect stronger than others.

The effect is directly proportional to the square of the electric field (where $|E|^2 = I$ is the intensity of light) and this leads to an intensity dependent refractive index (IRDI) in the material of

$$n(r) = n_0 + \frac{1}{2} n_2 I(r). \quad \text{Equation 11}$$

Equation 11 governs the optical Kerr effect where $n(r)$ is the overall refractive index, n_0 is the linear refractive index, n_2 is the second-order nonlinear refractive index and $I(r)$ is the intensity of the incident light.

Figure 12a is the intensity distribution of a regular Gaussian beam. Figure 12b shows the change in the index of refraction for a positive n_2 ; the index of refraction experienced by the beam is larger at the centre than at the sides.

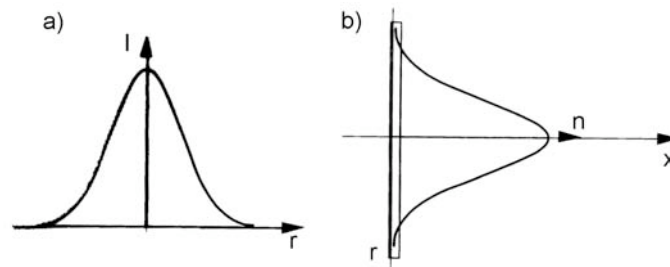


Figure 12⁽³⁶⁾ – a) is the intensity distribution of a regular Gaussian beam and b) is the variation of the index of refraction for $n_2 > 0$, which follows the intensity distribution along the diameter.

The index of refraction of a material has implications for the light passing through the material. The velocity of light in a material is equal to the speed of light in a vacuum divided by the index of refraction, n . Therefore the larger the value of n is the lower the velocity of light in the material becomes. Also n , according to Snell's law, defines the amount a beam will bend when it strikes a surface and if the velocity of light is different for different parts of the light beam then the beam will be reshaped or bent. This is known as refraction.

A lens is a common refractive element that is thicker in the middle than at the edges, causing the light to slow down more in the middle than in the edges. The light is focused towards the centre as it becomes bent inwards. In this case the lens has a constant index of refraction, n . However, altering n so that it is larger in the centre than at the edges will also bend light towards the centre and produce a lens.

Studying Equation 11 and Figure 12 highlight the fact that the light itself can alter the index of refraction. When the intensity of the light is high enough the electric field of the light becomes strong enough to distort the atoms of the material and change its refractive index. As the beam is more intense in the centre than the edges, the index of refraction becomes higher in the centre than at the edges, which causes the light to focus. A rod of material that acts like a lens for high intensity light based on the optical Kerr effect becomes known as a Kerr lens.

The focusing from the Kerr lens limits when the beam's diameter is narrow enough that its linear diffraction is large enough to balance out the Kerr effect (Figure 13). The effect is known as self-focusing.

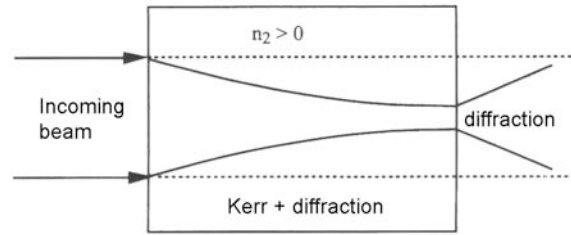


Figure 13⁽³⁷⁾ – The self-focusing of a laser beam in a medium with $n_2 > 0$.

The Kerr lens is only formed when the intensity of the light is extremely high, such as the instantaneous intensity of a mode-locked pulse. The weak intensity of a CW laser is not intense enough to induce an optical Kerr effect. This mechanism of only focusing the high intensity mode-locked pulses has been utilised for Kerr lens mode-locking.

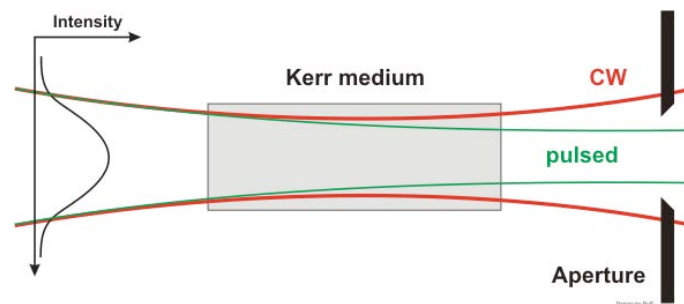


Figure 14⁽³⁸⁾ – Kerr lens mode-locking.

The self-focusing from the Kerr lens is means that the strong intensity maxima in laser cavity are focused much more strongly than the weaker maxima, which end up with negligible focusing.

The strong intensity maxima have now had their transverse structures reduced in size and so are less vulnerable to losses in the cavity, but the weaker intensities occupying a large volume experience enhanced losses. This leads to self mode-locking of the laser. Putting a slit or aperture into the system, as in Figure 14, increases the difference between the losses experienced by weaker intensity maxima and stronger intensity maxima by allowing most of the power of the stronger intensity maxima through, while heavily attenuating most of the weaker intensities. The diameter, position and shape of the slit must be calculated precisely.

The Mira Seed in the ULL adopts this type of saturable absorber mode-locking system to produce pulses around 20 fs in pulse duration (once a pulse compressor has been incorporated – currently 150 fs pulses are produced), each with around 3 nJ of energy. The repetition rate is 76 MHz and the central wavelength is 800 nm, most efficient for Ti:Sapphire. Currently, KLM Ti:Sapphire lasers can produce pulses of 6 fs duration⁽³⁹⁾ due to their very fast response time and no special saturable absorber medium requirements.

Problems In Kerr Lens Mode-Locking

KLM lasers can have start-up problems, meaning that the pulse formation does not begin without a helping hand. While there are no intensity fluctuations to create a significantly strong Kerr lens effect, the CW wave regime will prevail. Scottish scientists noticed that a Ti:Sapphire laser runs in continuous wave output and went into a pulsed regime once they banged on the table where the laser was mounted. The output then comprised of very short pulses and maintained itself once it had been initiated. This was the reason for the term ‘magic mode-locking’.

In normal operation, Ti:Sapphire lasers have one or two longitudinal modes operating simultaneously due to the atoms in the gain medium only emitting light at the same frequency of the stimulating light. So the earliest light to reach high intensity through amplification in the gain medium will establish the frequency for all subsequent light. Figure 7 showed how high intensities are gained when the laser operates over as many longitudinal modes as possible. With this in mind it is important to note that the modes can be wavelength shifted by changing the cavity length. If the length is changed rapidly enough there will be new modes oscillating and a transient condition, under which the laser output contains more modes than normally possible, is born.

When the number of modes lasing is large enough the peak intensities become high enough to start the Kerr lens mode-locking process. Once the mode-locking has begun it will continue without the need to rapidly change the cavity length. By giving a quick jolt to one of the mirrors by banging on the table, or shaking the mirrors using a starting mechanism, an intense pulse will result.

Group Velocity Dispersion

An ultrashort pulse of light will lengthen after it has passed through glass as the index of refraction, which dictates the speed of light in the material, depends nonlinearly on the wavelength of the light. The wavelength of an ultrashort pulse of light is formed from the distribution of wavelengths either side of the centre wavelength with the width of this distribution inversely proportional to the pulse duration.

At a given wavelength, the refractive index determines the velocity of a single mode, known as the phase velocity. Figure 15 is a plot of refractive index, $n(\lambda)$, versus wavelength, λ , and it sees $n(\lambda)$ decrease monotonically as λ increases, with a gradual upward curvature for most materials that are transparent in the optical spectrum. This is called dispersion. A material producing a downward curvature is said to have anomalous dispersion.

The slope of the curve, $\frac{dn(\lambda)}{d\lambda}$, is the group velocity, which defines the velocity of the wave packet with a central wavelength of λ . The second derivative of the slope, $\frac{d^2n(\lambda)}{d\lambda^2}$, yields the group velocity dispersion (GVD), which is defined as the rate that the frequency components of the wave packet change their relative phases. Group velocity dispersion is responsible for a dispersive broadening of the pulses.

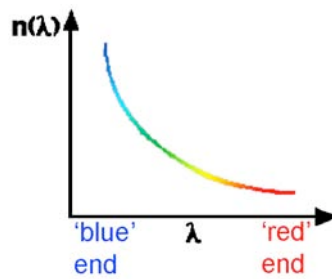


Figure 15⁽⁴⁰⁾ – Group velocity dispersion curve.

Self Phase Modulation

The optical Kerr effect is responsible for the nonlinear effect of self phase modulation (SPM). Each of the different frequency components of the pulse experiences a different phase shift, generating new frequencies and broadening the frequency spectrum of the pulse symmetrically. The leading edge of the pulse is shifted to lower frequencies (down chirp) while the trailing edge is shifted to higher frequencies (up chirp). The centre of the pulse experiences an approximate linear chirp.

Self phase modulation itself is not a dispersive effect, but it causes a pulse to no longer be transform-limited when crossing a transparent material, which means the pulse is then subject to dispersion, like that in Figure 16. Dispersion causes the ‘redder’ parts of the pulse to have a higher velocity than the ‘bluer’ parts, forcing the front of the pulse to move quicker than the back, temporally broadening the pulse. In anomalous dispersion the opposite is true and the pulse temporally compressed. The self phase modulation becomes stronger as the pulse becomes more intense, in turn causing more broadening.

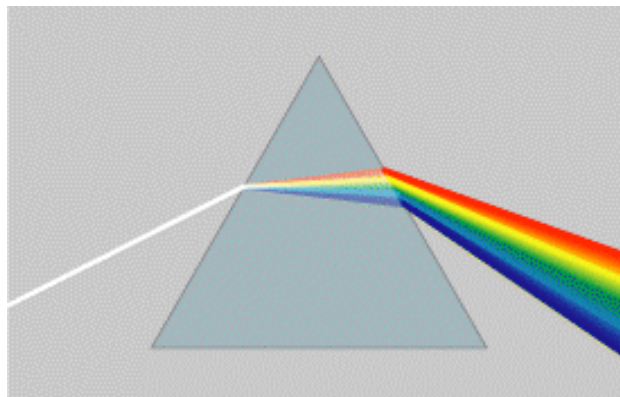


Figure 16⁽⁴¹⁾ – Dispersion of light through a prism.

Compensation

There are many dispersive elements within a laser cavity. An oscillating pulse will receive a slight chirp from each of these dispersive elements every round-trip. The cumulative effect from a lack of compensation for both GVD and SPM effects would see a temporal broadening for the pulse.

The Mira Seed oscillator uses a pair of prisms that the light passes through twice for complete compensation against the positively chirped dispersion an ultrashort pulse experiences on a round-trip. The choice of a material, orientation and distance between the prisms is such that they introduce a net negative GVD, cancelling out the positive GVD from the rest of the system.

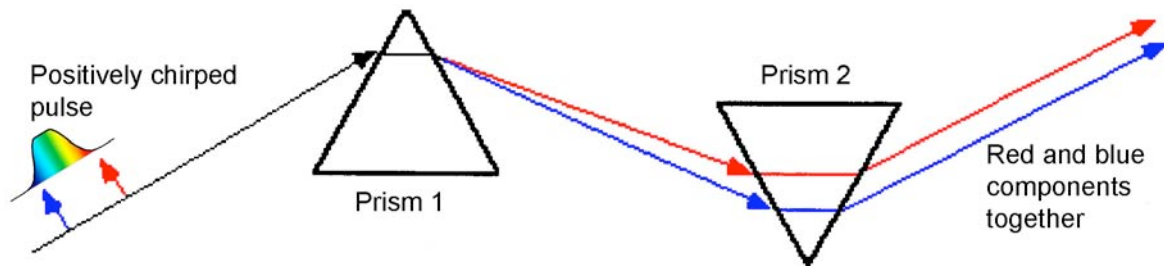


Figure 17⁽⁴²⁾ – Group velocity dispersion compensation.

Group velocity dispersion compensation, Figure 17, works as follows:

1. A pulse eventually forms and travels back and forth through the cavity. It is chirped by the self phase modulation in the Ti:Sapphire medium and by GVD from the other components in the cavity such as beam splitters and mirrors.
2. The chirped pulse enters prism 1 and the beam spreads as it is then diverted towards prism 2. As Figure 16 shows a prism disperses different wavelengths of light into different angles, due to the wavelength dependent changes in refractive index in the prism.
3. The blues are refracted more than the reds indicating that the blues travel faster than the reds. The system has introduced a negative GVD.
4. The magnitude of this created GVD can be controlled by the amount of glass in the prism. The overall system GVD of zero is achieved by orientating the prisms so the light travels through either more or less of the glass.

Compensation is important if sub-picosecond pulses are to be obtained. Figure 18 shows this graphically.

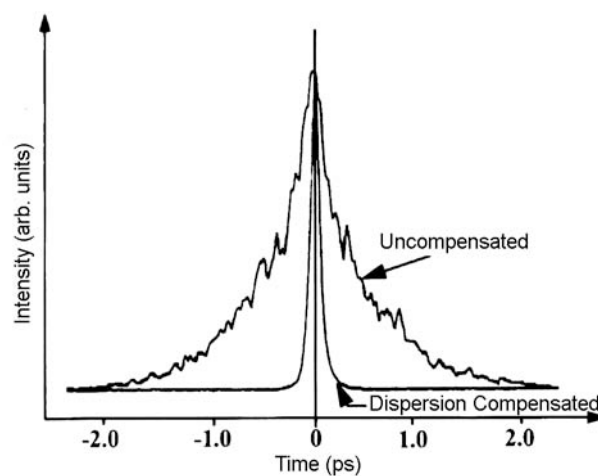


Figure 18⁽⁴³⁾ – An illustration of the effect of group velocity dispersion compensation on the pulse duration.

Eventually the pulse oscillating the cavity reaches equilibrium where it is the same shape after each round-trip. This balance between nonlinear and dispersive effects earns the pulses the label of solitons.

Figure 19 incorporates all of the above-mentioned parts to give a schematic of the Mira Seed oscillator. The pump beam from the Verdi V5 enters the oscillator from the left and is directed via a lens (L) and mirror (M) towards the Ti:Sapphire crystal. The starter is a pair of mirrors, needed to initiate the self mode-locking process. Various other mirrors divert the pulse through the cavity where it encounters the two prisms (BP) that compensate for dispersion. The slit allows only narrow beams of high intensity light to pass through to the output coupler, which allows some of the pulse to pass through to form the laser output and reflects the rest back for another round-trip of the system.

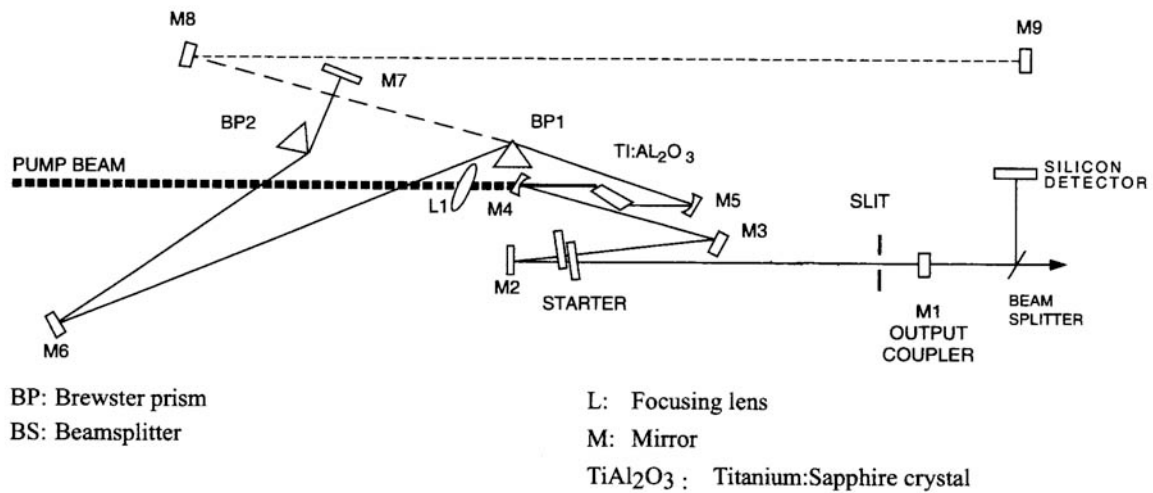


Figure 19⁽⁴⁴⁾ – Schematic of the Mira Seed Optical Laser.

Manipulation – Further Amplification

The pulses output from the oscillator are 20 fs in duration (once optimised) but only have 3 nJ of energy per pulse. Further amplification is needed for the pulses to carry more energy. This further amplification is based on the same principle of population inversion, which means an external source of radiation is needed to pump the gain medium in an amplifier.

Using J_{sat} as the intrinsic parameter called saturation fluence and τ_f as the fluorescence lifetime of the laser medium, the saturation intensity can be calculated using Equation 12.

$$I_{\text{sat}} = \frac{J_{\text{sat}}}{\tau_f} \quad \text{Equation 12}$$

The physical length of the amplifier medium is irrelevant and only the amount of energy stored in the amplifier medium is of interest. Table II shows two distinct groups of amplifier medium. The gases and liquids have a low J_{sat} while the solids have a much larger J_{sat} .

Amplifier Medium	J_{sat}
Dyes	$\sim 1 \text{ mJ/cm}^2$
Excimers	$\sim 1 \text{ mJ/cm}^2$
Nd:YAG	0.5 J/cm^2
Ti:Al ₂ O ₃	1 J/cm^2 at 800 nm
Cr:LiSAF	5 J/cm^2 at 830 nm
Nd:glass	5 J/cm^2
Yb:YAG	5 J/cm^2
Yb:glass	100 J/cm^2

Table II⁽⁴⁵⁾ – The saturation fluences of some typical amplification media used in amplifying ultrashort pulses.

Dye amplifiers were first used but they have major disadvantages in that they are only about 0.1% efficient and have a high optical gain. Amplified spontaneous emission (ASE) is the term for spontaneously emitted photons that follow the same optical path as a pulse and then undergo the same amplification. Amplified spontaneous emission limits the gain available in the medium and increases the noise, corresponding to an output from the amplifier of a short amplified pulse on top of a broad base. Generally, ASE accounts for 5-10% of the total energy output when using a dye amplifier. Excimers as amplifiers have the same drawbacks as dyes.

Solid-state materials have a much larger saturation fluence, meaning a much smaller optical gain per pass in the amplifier than dyes or excimers, greatly reducing the likelihood of ASE. For all the energy in the medium to be extracted multiple passes through the amplifier are required and two techniques have been designed to achieve this.

Multipass Amplification

The different passes in a multipass amplifier are separated geometrically as seen in Figure 20. However, the greater the number of passes needed the more complex the design must be. The design is limited also in the difficulty of focusing each pass through the gain medium. Typically four to eight passes are made, with cascading multipass amplifiers used for a greater number of passes. The technique is desirable as it is relatively inexpensive, but it needs time-consuming adjustments. The gain medium must also be used close to the damage threshold to have a high gain per pass ratio. However, it is capable of producing energies of above 50 mJ per pulse.

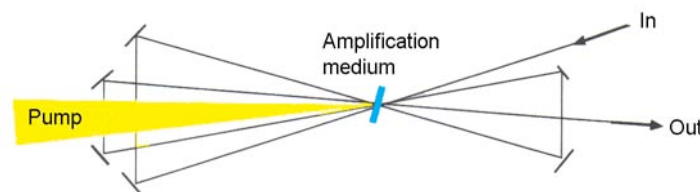


Figure 20⁽⁴⁶⁾ – A typical multipass amplifier set-up.

Regenerative Amplification

The passes in this method all follow the same path as the pulse is trapped in the resonator until it has extracted all the energy stored in the medium. The gain per pass becomes irrelevant in this case. The pulse is trapped using a Pockels cell and a broadband polariser. Figure 21 is a typical set-up of a regenerative amplifier. Firstly the gain medium is pumped so that it accumulates energy, then a pulse is injected into the cavity through a Pockels cell. A voltage is applied to the Pockels cell and its polarisation switches to trap the pulse in the resonator. The pulse then oscillates the cavity and after many round-trips is amplified to a high energy. Finally, another voltage is applied to the Pockels cell to switch its polarisation back and allow the pulse to leave the cavity.

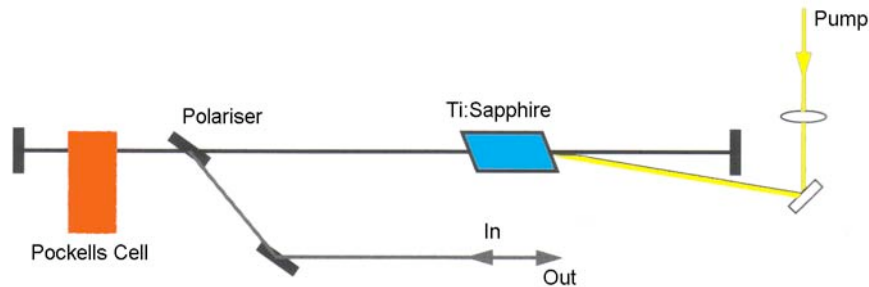


Figure 21⁽⁴⁶⁾ – A typical regenerative amplifier set-up.

Figure 22 is a typical picture of the pulse energy after a number of passes in a regenerative amplifier. Good efficiencies can be obtained from regenerative amplifiers.

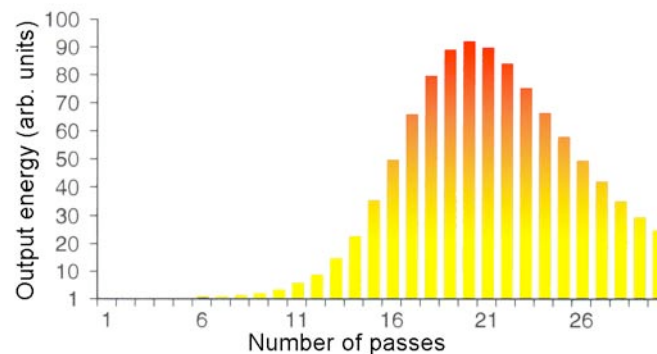


Figure 22⁽⁴⁷⁾ – The evolution of the pulse energy after a number of passes in a regenerative amplifier.

Table III lists some of those materials that can be used in a femtosecond amplifier. The bandwidth is an important feature and must be broad enough to support the pulse spectrum. Gain narrowing plays a vital role when amplifying ultrashort pulses. After each pass the wavelengths at the peak of the pulse are amplified more than those on the wings, leading overall to a relative reduction of the wings compared to the centre of the spectrum. In comparison the 50 nm bandwidth used in the oscillator is reduced to around 30 nm in the amplifier due to gain narrowing.

In addition to requiring a large bandwidth in the amplifier the other problem is the high fluence used by the amplifiers, which in ultrashort pulses leads to intensities greater than the damage threshold of the amplifier (of the order of 10 J/cm^2). Nonlinear effects such as

self-focusing in the gain medium cause the damage. To overcome this difficulty the technique of chirped pulse amplification (CPA) is used.

Gain Material	Bandwidth
Ti:Sapphire (Ti:Al ₂ O ₃)	650 – 1100 nm
Alexandrite (Cr:Be ₂ O ₃)	700 – 820 nm
Colquirites (Cr:LiSAF, Cr:LiCAF, etc.)	800 – 1000 nm
Fosterite	1250 – 1300 nm
Yb doped materials	1030 – 1080 nm
Glasses (Nd:glass)	1040 – 1070 nm

Table III⁽⁴⁸⁾ – A list of materials that can be used the medium in a femtosecond amplifier.

Figure 23 schematically shows how a chirped pulse amplification system operates. At first, a pulse is stretched by a large factor, usually somewhere of the order of 10^4 , so that its peak power is reduced considerably. The pulse is then amplified safely within the damage threshold of the amplifying medium before finally being recompressed back to approximately its original duration.

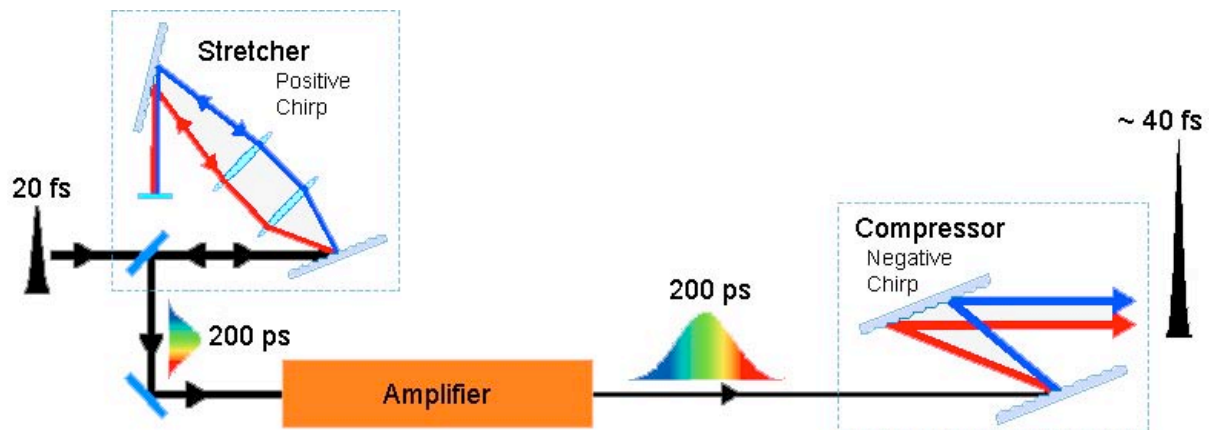


Figure 23⁽⁴⁹⁾ – Diagram of chirped pulse amplification relevant to the pulse durations in the Legend regenerative amplifier at the ULL.

The stretcher is a pair of gratings separated with an afocal system of magnification, making the red optical path shorter than the blue. Once the pulse has passed the stretcher its duration is of around 200 ps. The pulse is trapped in the cavity and is amplified on each pass through the gain medium. Once the pulse saturates the gain and reaches the maximum energy (see Figure 22) it is extracted from the amplifier and sent to the compressor where its initial duration is recovered. It is possible at this point to have pulse of 30 fs with energies in the joule range, equating to a peak power of over 10 TW (more than the total electrical power produced on Earth⁽⁵⁰⁾ – for that 30 fs anyway). The efficiency is around 100 times greater than dye amplifiers at above 10% and when the pulses are focused intensities of 10^{19} W/cm² are possible.

However there are problems with chirped pulse amplification and these lie with the difficulty in recovering the initial pulse duration and quality. The compressor must compensate for the dispersion introduced not only from the stretcher but from the amplifier too, so the distance between the gratings must be set to a larger value in the compressor than the stretcher. It is possible to overall cancel out the second-order dispersion and obtain

relatively short pulses, but extra care and design must be employed to keep higher-order dispersion terms, translated as wings and pre-pulses from degrading the final pulse quality.

Appendices A and B are photos and brief descriptions of two phenomena directly output from the femtosecond regenerative amplifier. These are laser induced air breakdown and white light continuum generation.

The ULL – Optical Pump 2

To supply the power to the amplifier in the ULL the Coherent Evolution-30, a Q-switched, frequency doubled, neodymium-doped yttrium lithium fluoride (Nd:YLF) laser, is used. The Evolution-30 produces pulses of duration 120 ns at 527 nm with a repetition rate of 1 kHz. The power output is 20 W giving each pulse 20 mJ of energy. Nd:YLF lasers have good beam quality due to their low noise, are compact (see Figure 24a), stable and very reliable thanks in part to the 10,000 hour lifetime of the diode pump. The range of power levels that are available make them ideal for pumping ultrafast Ti:Sapphire amplifiers.

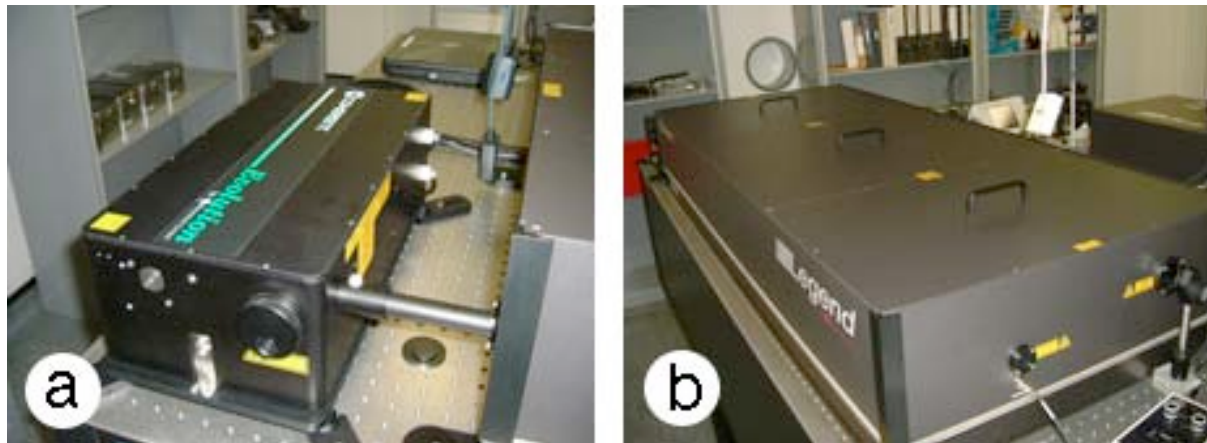


Figure 24 – a) Evolution-30 Nd:YLF pump laser and b) Legend USP-High Energy femtosecond regenerative amplifier.

The ULL – Regenerative Amplifier

The ULL uses the Coherent Legend USP-High Energy regenerative amplifier (Figure 3.4 and Figure 24b) to bring the (optimised) 20 fs, 3 nJ pulses from the oscillator to 35 fs (currently producing durations of 65 fs), 2.5 mJ pulses, increasing the energy by 6 orders of magnitude. The energy for the Ti:Sapphire gain medium comes from the Evolution-30 pump laser in the form of 20 mJ pulses at 120 ps duration. The repetition rate of the pump is 1 kHz, which differs greatly from the repetition rate of 76 MHz for the femtosecond pulses from the oscillator.

To solve this problem only 1 pulse (in every 76,000) is selected from the oscillator pulse train each time the energy in the Ti:Sapphire gain medium is maximised by the pump beam (1,000 times every second). The selected pulse is injected into the cavity and allowed to oscillate by the regenerative amplifier until it has the maximum possible energy.

The Legend USP-High Energy is used in the ULL as it perfectly accompanies the Mira Seed oscillator, allowing the output pulse to be sub 40 fs in duration (at 800 nm) with a

peak power of 80 GW. It contains a stretcher and compressor grating system, which can compensate for the higher-order errors introduced by the amplification process giving a superior beam quality. The design is compact and simple using a regenerative system, instead of a complex multipass design, with the largest part of the amplifier being the pulse recompression gratings.

Measurement

The characterisation of ultrashort pulses has always been a challenge and for many years it was possible to create them but not to measure them. A full characterisation is needed to fully determine experimental conditions before the pulses are used for experiments. Measurements can be made to find the energy (or power), shape, duration and spectrum of the pulse. Characterising ultrashort laser pulses has proved difficult, as the photodetectors used to detect longer pulses are not fast enough to use with ultrashort pulses.

The electric field of a pulse can be specified as a function dependent on time or dependent on spatial position and a product of the two functions can give the whole spatiotemporal profile of the electric field of a pulse. However, a pulse produced from Kerr lens mode-locking show signs of significant coupling of both spatial and temporal properties (it has a time-dependent beam radius), making a complete pulse characterisation very tricky.

Although the pulse energy can be measured directly or calculated from the average power and repetition rate, and the pulse power can be found using a photodiode, a complete pulse characterisation in one step is much more beneficial. A complete characterisation will reveal the variation of the electric field with time or the complex spectrum, which includes the spectral shape and phase. The two most common and indirect techniques are frequency resolved optical gating (FROG) and spectral interferometry for direct electric field reconstruction (SPIDER).

These indirect approaches make use of correlation functions. There are two key points to these techniques; the first being that a light pulse takes a picosecond to travel 300 microns in air – a length that is easy to measure and calibrate. Secondly, the correlation function says that starting with two time-dependent functions $F(t)$ and $F'(t)$ with one being known, say $F(t)$, the measurement of $G(\tau)$ will directly give the other, $F'(t)$. Where τ is the delay $G(\tau)$, the first-order correlation function, is defined as⁽⁵¹⁾

$$G(\tau) = \int_{-\infty}^{+\infty} F'(t)F(t - \tau)dt. \quad \text{Equation 13}$$

To measure an event in time a shorter event is required. So for pulses of an ultrashort duration the pulse is used to measure itself and autocorrelation is the result. The basic principle is to split the pulse using a beam splitter to generate two copies and variably delaying one with respect to the other. The copies are then spatially overlapped in an instantaneous nonlinear medium, such as a second harmonic generation (SHG) crystal. The SHG crystal produces a signal at twice the frequency of the incoming light with an envelope given by

$$E(t, \tau) \propto E(t)E(t - \tau). \quad \text{Equation 14}$$

Considering Equation 13 and Equation 14 the field has an intensity proportional to the product of the intensities of the two pulses,

$$I(t, \tau) \propto I(t)I(t - \tau). \quad \text{Equation 15}$$

Detectors are too slow to measure Equation 15, but will instead measure the intensity autocorrelation, given in Equation 16.

$$A(\tau) = \int_{-\infty}^{+\infty} I(t)I(t - \tau)dt \quad \text{Equation 16}$$

The autocorrelation trace is obtained by graphing the SHG energy against the delay. The experimental set-up of an intensity autocorrelator is demonstrated in Figure 25.

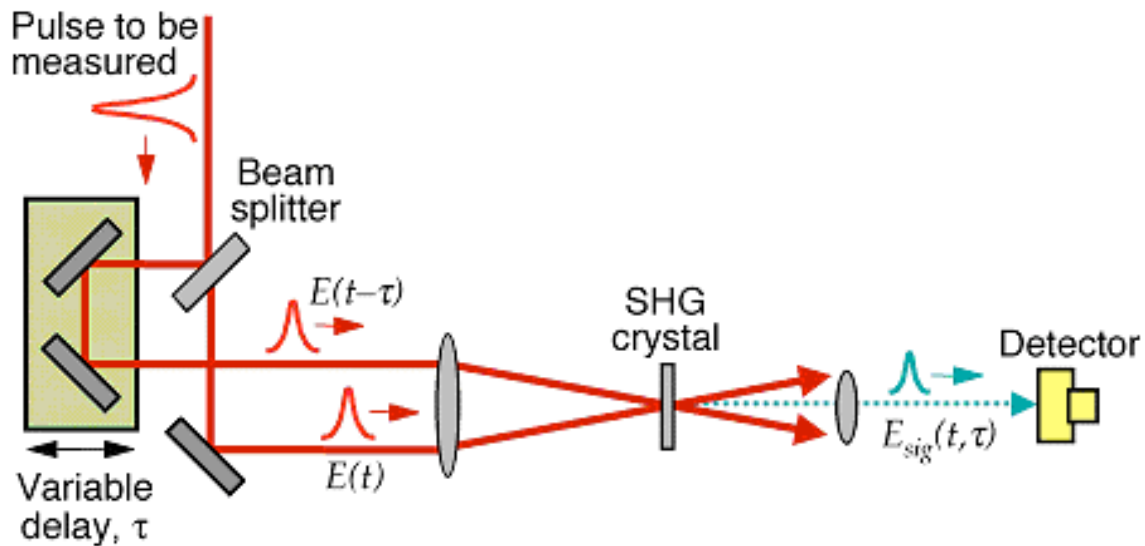


Figure 25⁽⁵²⁾ – The experimental set-up of an intensity autocorrelator with second-harmonic generation.

However, autocorrelation doesn't always yield the pulse intensity because different intensities can have the same autocorrelation and autocorrelations are always symmetric about the centre, even for an asymmetric pulse shape. Figure 26 shows these disadvantages, with the last row displaying the symmetric autocorrelation despite a pre-pulse in the original pulse. Autocorrelation also does not measure any spectral resolution.

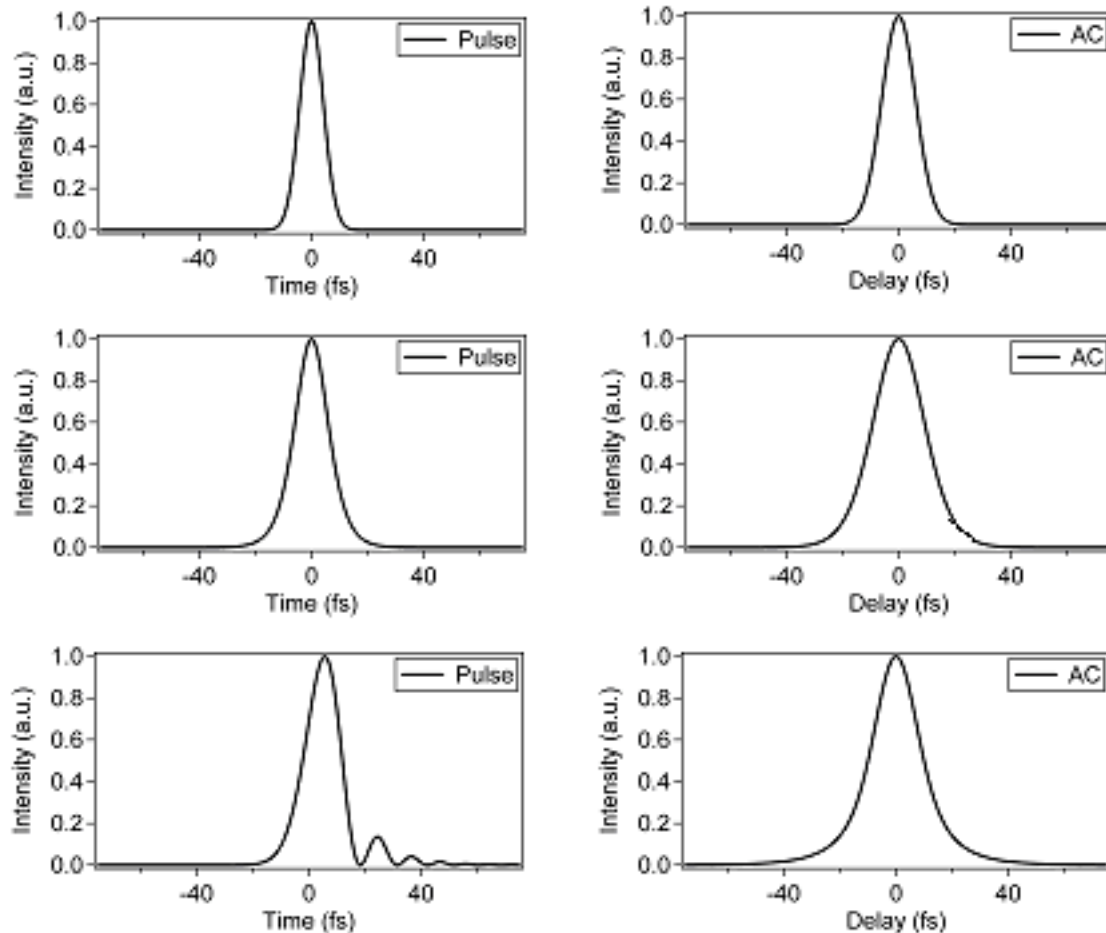


Figure 26⁽⁵³⁾ – Some examples of pulse intensities and their autocorrelations.

FROG

Frequency resolved optical gating (FROG) still uses the pulse to measure the pulse itself, but operates in the time-frequency domain. Measurements in this domain involve temporal and frequency resolution simultaneously, such as on a musical score. Figure 27 is a ‘scale’ or ‘linearly chirped pulse’ with frequency plotted against time. On the top is intensity, beginning with low intensity (*pianissimo*), up to high intensity (*fortissimo*) and back down to low intensity. The score is a function of time as well as frequency.



Figure 27⁽⁵⁴⁾ – A musical score, known as a scale, is a plot of frequency against time with information above it about the intensity.

FROG is similar to autocorrelation measurements but involves measuring the signal spectrum versus the delay instead of signal energy versus delay. The most common and sensitive version of FROG is second harmonic generation (SHG) FROG, in which a doubling crystal is used. The FROG trace is measured in the (ω, τ) plane, which when projected along the frequency axis gives the autocorrelation function. An iterative algorithm then retrieves the amplitude and phase of the incident laser pulse.

In SHG FROG (Figure 28), the frequency-doubled light of the autocorrelation is the signal beam given by Equation 14. The signal is imaged onto the slit of a spectrometer, where the time delay (τ) between the two replica pulses is parameterised along the slit⁽⁵⁵⁾. The spectrometer then disperses the light perpendicular to the slit, producing a 2D image with delay time and frequency as the axes. The intensity is detected by a CCD (charge-coupled device) array,

$$I_{FROG}(\omega, \tau) = \left| \int_{-\infty}^{+\infty} E_{sig}(t, \tau) \exp(i\omega t) dt \right|^2. \quad \text{Equation 17}$$

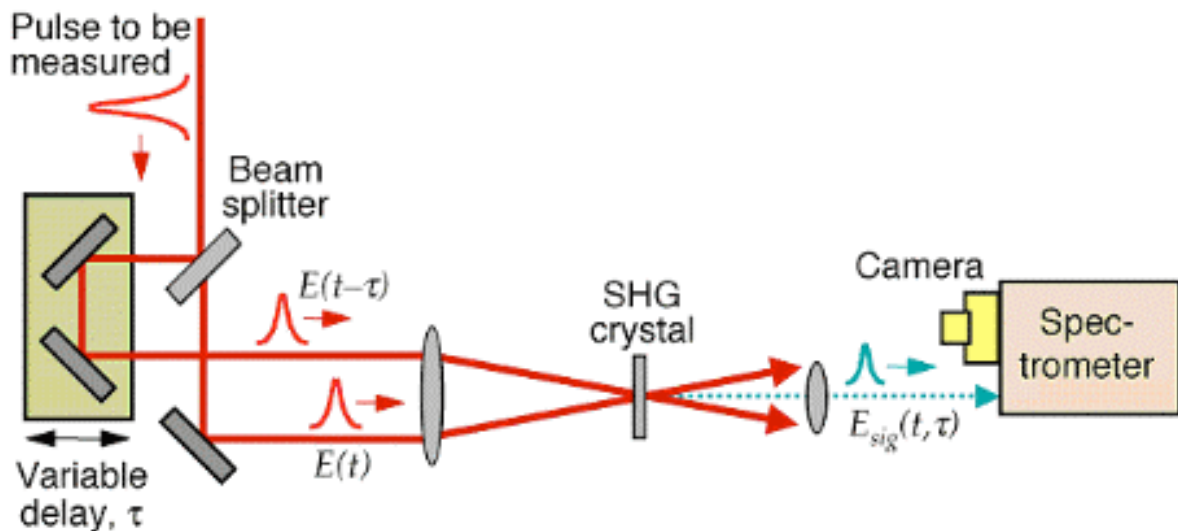


Figure 28⁽⁵⁶⁾ – The set-up of SHG FROG. The measured pulse is split into two replica pulses, which are then focused in a nonlinear optical medium creating a signal field (as in autocorrelation). The signal pulse is spectrally resolved.

FROG does not measure the absolute phase of a pulse nor does it give an absolute time reference as the pulse is measured with itself. There is also ambiguity in SHG FROG as a pulse and its time-reversed replica are both possible. FROG can also have complexity, size, cost, maintenance and alignment issues.

GRENOUILLE

GRENOUILLE (grating eliminated no-nonsense observation of ultrafast incident laser light E-fields) is the result of a simplification in the FROG technique. A Fresnel biprism (a prism with an apex close to 180°) replaces the beam splitter and the delay line and a thick doubling crystal acts as the nonlinear time-dating element and the spectrometer. The spectral resolution comes from angular resolution of the output light of the crystal. The amplitude and phase of the laser light come from using the FROG algorithm (befitting as grenouille is French for frog) and the trace is directly formed on a CCD camera.

SPIDER

SPIDER is the acronym for spectral interferometry for direct electric field reconstruction and is a competing ultrashort pulse measuring technique to FROG. SPIDER is a similar concept to autocorrelation, but instead of gating a pulse with a time-delayed replica of itself the pulse is interfered with a frequency-shifted (spectrally sheared) copy of itself. SPIDER then uses a nonlinear mixing as a combination of filters to produce a signal that can be measured by a slow (in comparison to the pulse duration) detector. The technique is essentially based on the measurement of the interferences between different frequencies of the spectrum of the pulse.

The set up of SPIDER is seen in Figure 29. The generated chirped pulse is usually part of the incident pulse, which goes into a dispersive delay line such as a block of dispersive material or a grating pair. The generation of the two replica pulses is normally achieved with a Michelson interferometer or a glass etalon, each of which can provide the delay required between the pulses. All three pulses meet in a nonlinear (SHG) crystal. The technique is essentially based on the measurement of the interferences between different frequencies of the spectrum of the pulse.

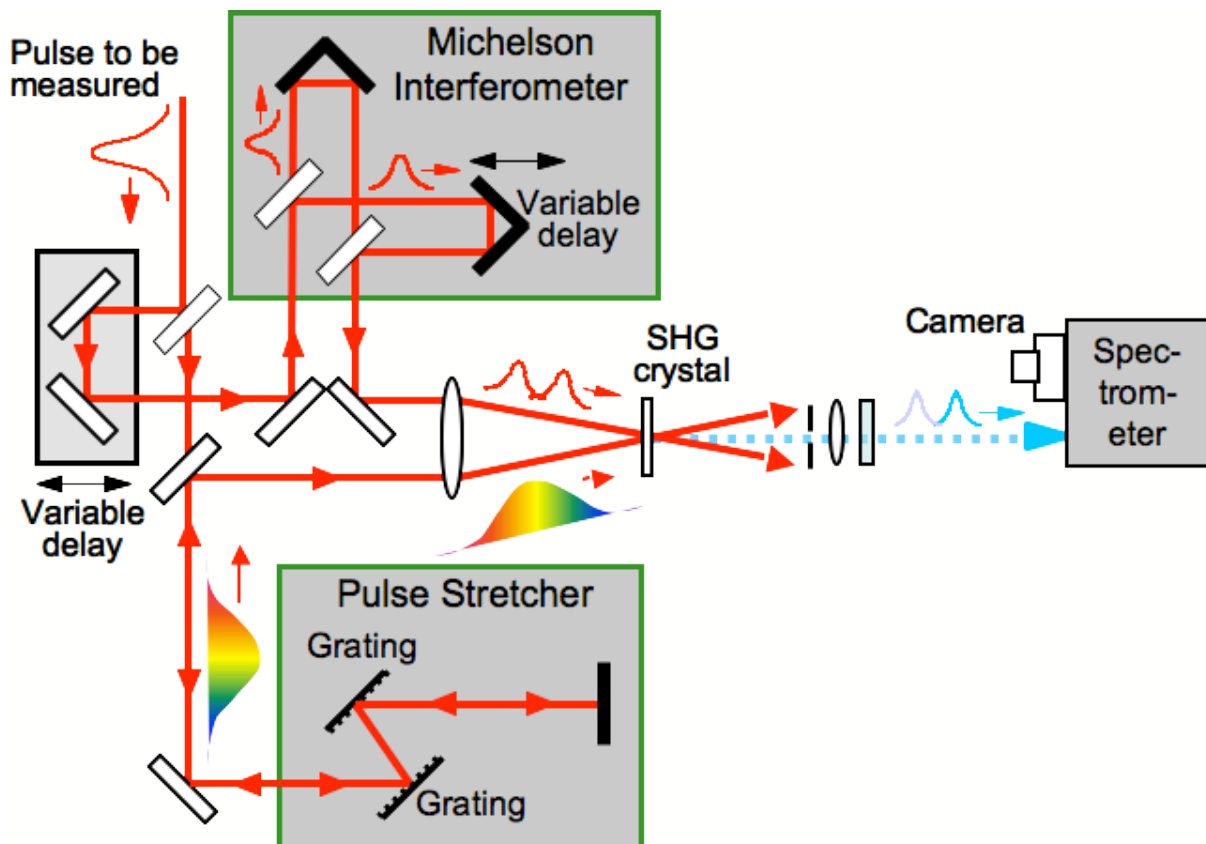


Figure 29⁽⁵⁷⁾ – The main elements in a SPIDER set-up.

Performing spectral interferometry of a pulse with itself sees the spectral phase cancel out as perfect sinusoidal fringes always occur. However, performing sum-frequency generation (SFG) between a heavily chirped pulse and two time-separated replicas of the incident pulse in a nonlinear medium will frequency shift one replica relative to the other. The two up-shifted pulses will yield the derivative of the spectral phase, providing the delay between the pulses is larger than the pulse duration. Figure 30 is a closer inspection of the combination of all three pulses in a SHG crystal.

The phase difference between the two sheared replica pulses is extracted using algebraic methods. A fast Fourier transform, a filtering of one of the interference terms and a final fast Fourier transform will reveal the phase difference. The phase of the initial pulse is gained using an inversion algorithm that is totally algebraic.

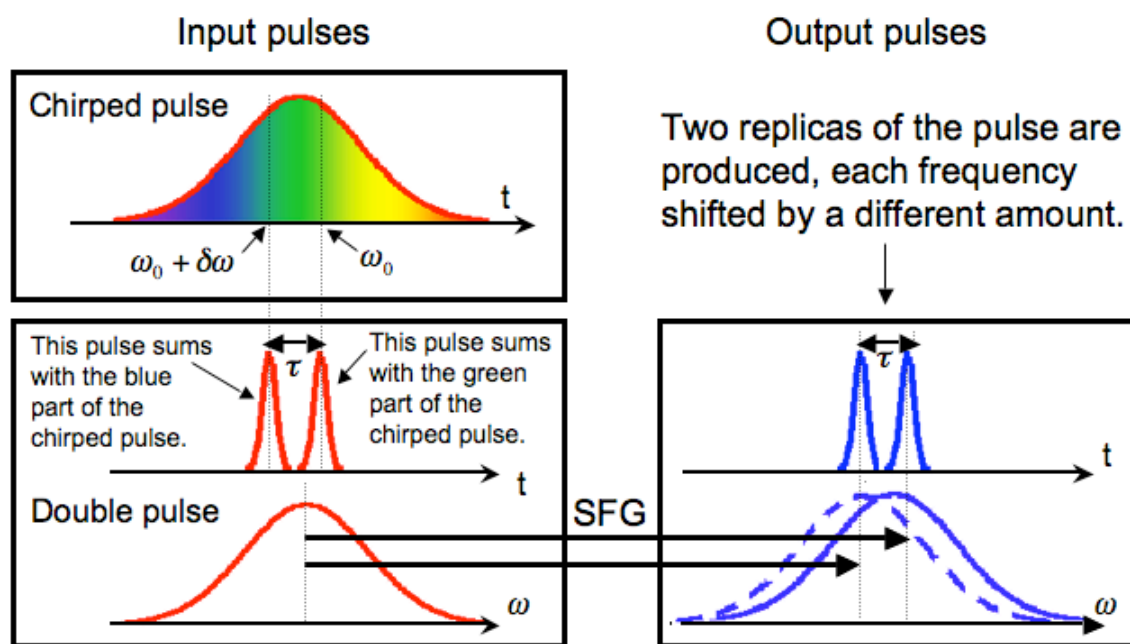


Figure 30⁽⁵⁷⁾ – The generation of two sheared replicas of the input pulse from a nonlinear interaction with a chirped pulse.

The ULL uses SPIDER to measure its pulses (Figure 31a) and its advantages include the real-time pulse retrieval and low sensitivity to noise, as no iterative algorithm is required, just algebraic operations. Minimal initial data is required and a single shot will yield the experimental trace. The costs are lower as it involves no moving parts and only a 1D spectrometer is required. However, the apparatus contains a lot of sensitive alignment parameters making it complex and a poor beam quality can wash out the fringes preventing a measurement.

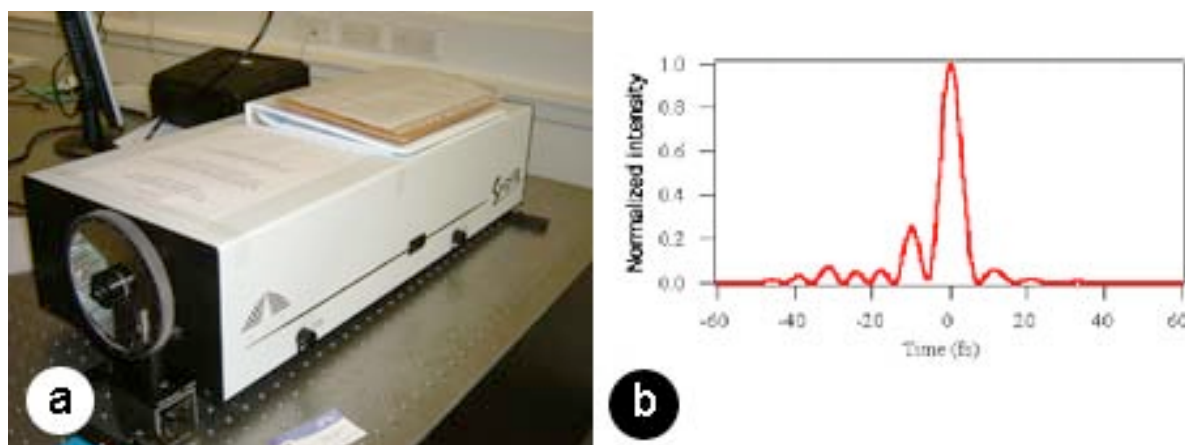


Figure 31 – a) The SPIDER (Spectral Interferometry for Direct Electric Field Reconstruction) at the Ultrafast Laser Laboratory used to characterise ultrashort optical pulses and b) ⁽⁵⁸⁾ a 5.9 fs pulse from a Ti:Sapphire mode-locked oscillator measured using SPIDER.

Figure 31b shows what can be obtained from SPIDER, a 5.9 fs pulse that is the shortest yet characterised using SPIDER ⁽⁵⁹⁾.

Applications

There are far too many uses for ultrashort laser pulses to name in full here. Prof. Ursula Keller manages to list just some of the current applications of ultrashort laser pulses ⁽⁶⁰⁾. The ultrashort pulse duration allows for a fast temporal resolution, in a similar way that a strobe light appears to freeze the motion of people. A mode-locked laser is able to do the same with objects such as molecules where A. H. Zewail was awarded the Nobel Prize in 1999 for his work in chemical reaction dynamics using mode-locked lasers ^(61,62).

The high repetition rate can be utilised for many different applications including high capacity telecommunications systems ^(63,64), photonic switching devices ⁽⁶⁵⁾ and in the future for clocks on large-scale integrated microprocessors ⁽⁶⁶⁾.

The broad spectrum associated with ultrashort pulses supports good spatial resolution for non-invasive cross-sectional imaging techniques such as optical coherence tomography (OCT) in biological systems ^(67,68). A 2D image is produced as a result of optical scattering from internal tissues. The pulse train of an oscillator output provides a stable comb-shaped spectrum with the spacing of the modes equalling the repetition rate. The broadband frequency comb has also been used recently in high precision optical frequency metrology, which acts as a ruler in the frequency domain ^(69,70). It is expected to be able to produce an all-optical atomic clock, outperforming today's caesium clocks ⁽⁷¹⁾.

The high peak intensity of pulse can be utilised to alter materials by cold ablation, meaning the material is changed from solid straight to gas without an increase in temperature. The quality of ablated holes using femtosecond intense ultrashort pulses is much higher than pulses of longer duration ^(72,73). In the medical field, a much higher precision of surgical cutting ⁽⁷⁴⁾ is observed, particularly in fields such as tumour removal ⁽⁷⁵⁾ or corneal surgery ⁽⁷⁶⁾. The damage to surrounding tissues is greatly reduced as the pulse duration decreases.

The Future

The field of ultrashort laser physics has existed for nearly four decades. It can be considered a fairly mature field and the generation, manipulation, measurement and usage of ultrashort pulses are at the frontiers of laser research today. There have been a number of developments since De Maria *et al*⁽¹⁷⁾ produced the first picosecond pulses, most of which has been included here.

Dr. Rüdiger Paschotta cites a number of ongoing developments to further the field of ultrashort laser pulse generation⁽⁷⁷⁾. Research into new gain media is in progress with the development of new crystal materials displaying interesting properties and superior performance. New ytterbium-doped gain media such as sesquioxides or tungstates could provide even higher powers in ultrashort pulses. Cr²⁺:ZnSe (chromium-doped zinc selenide) is expected to be suitable for the generation of pulses with a 20 fs duration in the near future.

Mode-locked fibre lasers have made huge advances over recent years and are being researched to replace bulky solid-state lasers in the future. Fibre lasers can generate high average powers and a good beam quality, however at present there is no fibre laser capable of replacing the Ti:Sapphire laser in the region of 700-1100 nm⁽⁷⁸⁾. At present fibre lasers are more expensive than their bulk laser counterparts, but due to the need for fewer mechanical parts they are hoped to become significantly smaller and cheaper.

Amplification devices for lower pulse repetition rates will become important for their uses in material processing, such as micromachining. The future progress in the field of ultrashort laser pulse generation can only unlock new applications.

Attosecond physics is just over the horizon. Currently Ti:Sapphire cannot be bettered as an ultrafast laser and it is KLM Ti:sapphire lasers that have produced pulses of 6 fs in duration⁽³⁹⁾. At 800 nm central wavelength an optical cycle lasts 2.7 fs, with two optical cycles making up a 5.4 fs pulse. Therefore to produce a cycle shorter than 1 fs extreme-ultraviolet (XUV) or x-ray wavelengths must be used⁽⁷⁹⁾. Atoms exposed to a strong femtosecond laser emit coherent XUV light at high-harmonics of the driving laser and at very high photon energies a series of attosecond XUV bursts are radiated, separated by half of the laser's oscillation period. Attosecond pulse generation is something that the ULL hopes to achieve in the near future with the goal of studying electron dynamics in mind.

The progress in the field of ultrashort laser pulse generation has been rapid and continuous, and has a long lifetime ahead. Laser powers should increase and intensities should be regularly pushed over 10^{21} W/cm². Research continues into discoveries for new gain media in the hope of improving on the excellent Ti:Sapphire and will continue for as long as ultrashort laser pulses remain useful, which judging by the numerous and varied applications, will be for many years to come. Of course, as the technology continues to develop more applications will be found for it. The lasers should become cheaper to build as technologies and design improve making them further compacted, and cheaper to buy as further applications call for them. Furthermore, the advent of attosecond physics, brought on by the development and usage of femtosecond pulses may finally allow us to see an electron's dynamics in orbit around an atom, much like a strobe allows us to see in 'slow motion' a dancer at a nightclub. Although the genesis of ultrashort laser pulse generation was not long ago, it is clear that it is shaping up for a long lifetime ahead.

Acknowledgements

This article has swiftly introduced the reader to laser basics whilst pointing to sources with more in-depth discussion, before going on to cover the generation, manipulation, usage and future of ultrashort laser pulses. I would like to thank Dr. O’Leary for supervising this project and demonstrating the Ultrafast Laser Laboratory in action. My thanks also go to Dr. Paschotta of RP Photonics for his personal communication about the future research goals in the field of ultrashort laser pulses.

Appendix A

Laser Induced Air Breakdown

With the laser beam focused through a lens down to a small spot size the electric field is high enough (above roughly 1 kV/mm) to cause a breakdown of air, much the same as lightning. The breakdown appears as a small, bright spark (Figure 32) but the understanding behind breakdown with optical pulses is not fully understood.

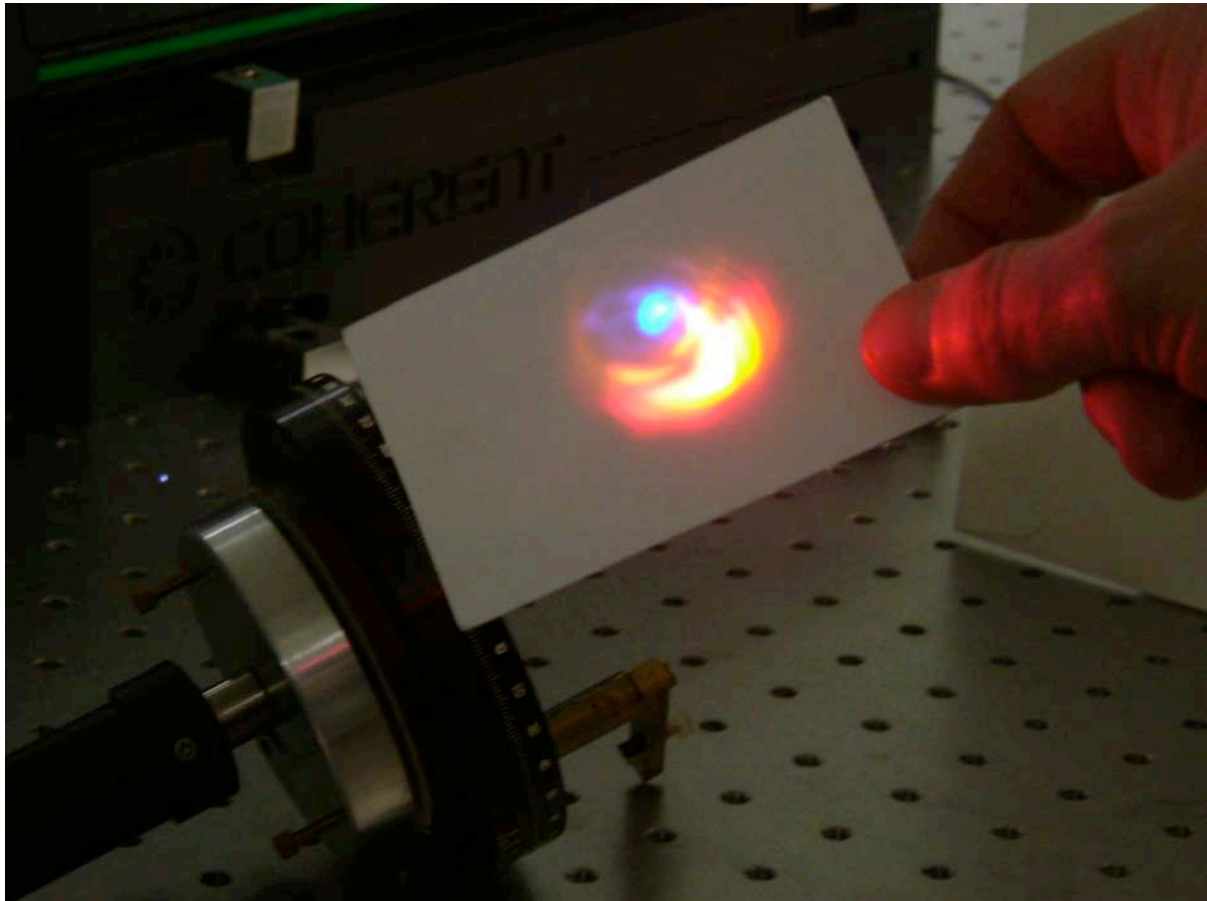


Figure 32 – Laser induced air breakdown in action. The left of the picture shows the spark where the air is ionised 1,000 times a second. The nonlinear effects are seen on the paper with the wavelengths of light dispersed making the light visible.

For femtosecond pulses it is believed that multiphoton ionisation efficiently generates free carriers in the initial phase of the pulse. The generated plasma then absorbs strongly, which leads to further heating, expansion and ionisation. The cycle repeats 1,000 times a second due to the output from the femtosecond regenerative amplifier at 1 kHz. The effect is also audible, as it occurs 1,000 times a second it is well within the human hearing range, and sounds like a medium-pitched whine.

Appendix B

White Light Continuum Generation

The main process in white light continuum generation is due to self phase modulation, which overall makes more wavelengths visible than were previously visible. The bluer wavelengths suffer more of a dispersive effect than the redder ones. Figure 33 shows how the bluer wavelengths of light are now visible due to a strong chirp from this effect.

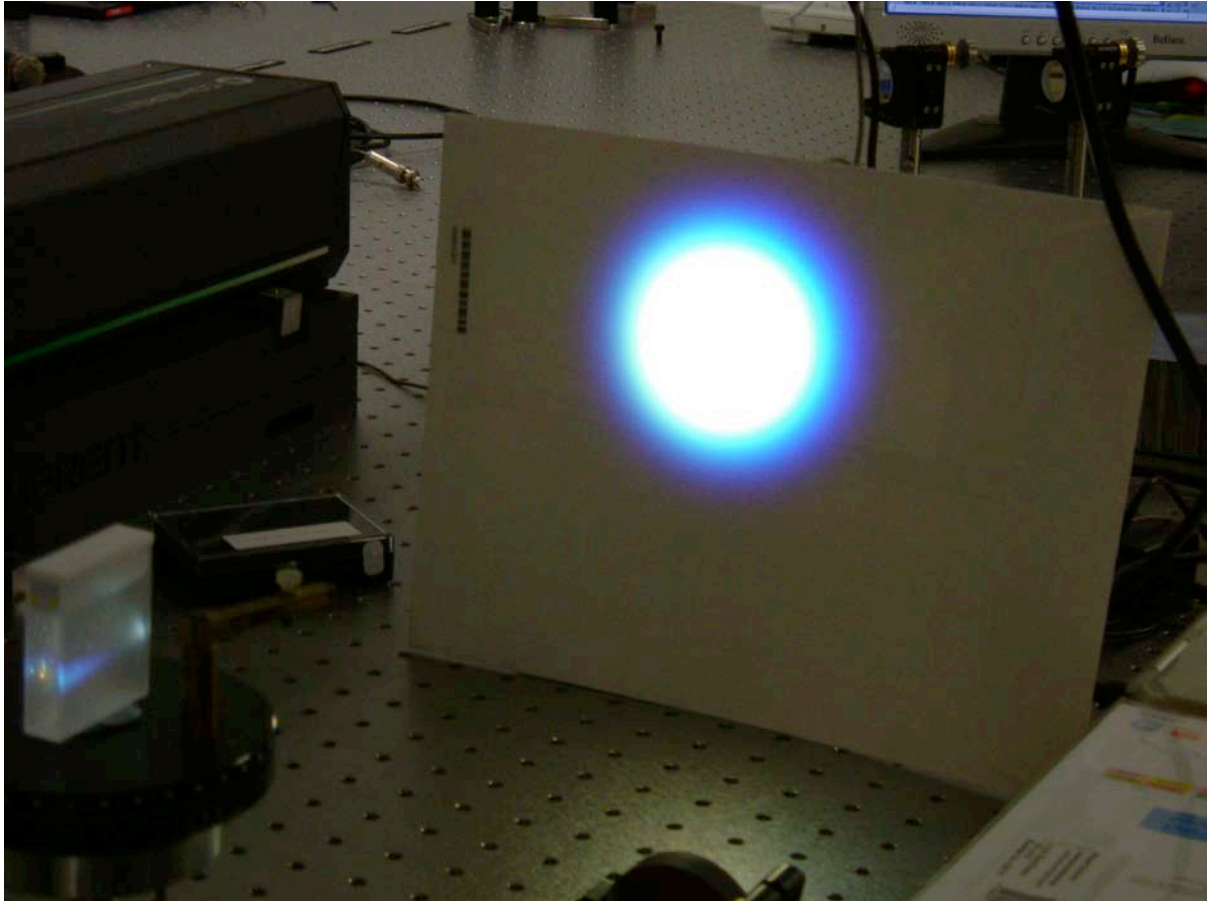


Figure 33 – The laser beam is focused into a cell of water and the effects of white light continuum generation are visible on the paper.

References

- ¹ Townes, C.H.; *A Century of Nature: Twenty-One Discoveries that Changed Science and the World*, University of Chicago Press, 2003
- ² <http://en.wikipedia.org/wiki/Image:Laser.svg>
- ³ Rullière, C.; *Femtosecond Laser Pulses: Principles and Experiments*, Springer, 2005, p. 4
- ⁴ Rullière, C.; *Femtosecond Laser Pulses: Principles and Experiments*, Springer, 2005, p. 1-23
- ⁵ Wilson, J.; Hawkes, J.F.B.; *Lasers: Principles and Experiments*, Prentice Hall, 1987, p. 1-34
- ⁶ <http://en.wikipedia.org/wiki/Lasers>
- ⁷ <http://nobelprize.org/physics/educational/laser/facts/index.html>
- ⁸ Frasninski, L.J.; *PH3713 Laser Principles and Applications*, course notes
- ⁹ <http://www.ull.reading.ac.uk/facilities.htm>
- ¹⁰ Moulton, P.F.; *Spectroscopic and laser characteristics of Ti:Al₂O₃*, J. Opt. Soc. Am. B 3, 1986, p. 125
- ¹¹ http://www.rp-photonics.com/titanium_sapphire_lasers.html
- ¹² <http://www.coherent.com/Lasers/index.cfm?fuseaction=show.page&ID=873&loc=301>
- ¹³ <http://www.coherent.com/Lasers/index.cfm?fuseaction=show.page&id=905&loc=301>
- ¹⁴ <http://www.coherent.com/Lasers/index.cfm?fuseaction=show.page&ID=879&loc=301>
- ¹⁵ <http://www.coherent.com/Lasers/index.cfm?fuseaction=show.page&id=902&loc=301>
- ¹⁶ <http://www.ape-berlin.de/pdf/Spider.pdf>
- ¹⁷ Maria, A.J., et al.; *Self mode-locking of lasers with saturable absorbers*, Appl. Phys. Lett. 8, 1966, p. 174–176
- ¹⁸ Rullière, C.; *Femtosecond Laser Pulses: Principles and Experiments*, Springer, 2005, p. 31
- ¹⁹ Image edited from <http://www.newastro.com/newastro/book/C2/images/FWHM.jpg>
- ²⁰ Rullière, C.; *Femtosecond Laser Pulses: Principles and Experiments*, Springer, 2005, p. 32
- ²¹ http://www.rp-photonics.com/saturation_power.html
- ²² Mira Seed optical laser manual
- ²³ Rullière, C.; *Femtosecond Laser Pulses: Principles and Experiments*, Springer, 2005, p. 20
- ²⁴ <http://en.wikipedia.org/wiki/Modelocking>
- ²⁵ <http://en.wikipedia.org/wiki/Image:Modelock-1.png>
- ²⁶ Rudolph, D.; *Ultrashort Laser Pulse Phenomena*, Academic Press, 1995, p. 209
- ²⁷ Rullière, C.; *Femtosecond Laser Pulses: Principles and Experiments*, Springer, 2005, p. 58
- ²⁸ http://www.rp-photonics.com/img/actively_ml_laser.png
- ²⁹ http://www.rp-photonics.com/img/active_mode_locking.png
- ³⁰ http://www.rp-photonics.com/img/passively_ml_laser.png
- ³¹ http://www.rp-photonics.com/img/passive_mode_locking.png
- ³² Keller, U.; *Recent Developments In Compact Ultrafast Lasers*, Nature, 424, 2003, p. 834
- ³³ Ishida, Y.; Sarukura, N.; Nakano, H; *Conference: Ultrafast Phenomena VII*, OSA, California, 1990
- ³⁴ Spence, D.E.; Kean, P.N.; Sibbett, W.; *Conference: lasers and electro-optics*, California, 1990
- ³⁵ Keller, U.; et al.; *Femtosecond Pulses From A Continuously Self-Starting Passively Mode-Locked Ti:Sapphire Laser*, Optics Letters, 16, 13, 1991, p. 1024
- ³⁶ Rullière, C.; *Femtosecond Laser Pulses: Principles and Experiments*, Springer, 2005, p. 47
- ³⁷ Rullière, C.; *Femtosecond Laser Pulses: Principles and Experiments*, Springer, 2005, p. 48
- ³⁸ http://upload.wikimedia.org/wikipedia/en/0/07/Kerr-lens_Modelocking.png
- ³⁹ Ell, R.; et al.; *Generation of 5-fs pulses and octave-spanning spectra directly from a Ti:sapphire laser*, Opt. Lett., 26, 6, 2001 p. 375

-
- ⁴⁰ Image edited from Mira Seed optical laser manual
- ⁴¹ http://upload.wikimedia.org/wikipedia/commons/0/06/Prism_rainbow_schema.png
- ⁴² Image edited from Mira Seed optical laser manual
- ⁴³ Rullière, C.; *Femtosecond Laser Pulses: Principles and Experiments*, Springer, 2005, p. 81
- ⁴⁴ Mira Seed optical laser manual
- ⁴⁵ Rullière, C.; *Femtosecond Laser Pulses: Principles and Experiments*, Springer, 2005, p. 180
- ⁴⁶ Image edited from Rullière, C.; *Femtosecond Laser Pulses: Principles and Experiments*, Springer, 2005, p. 182
- ⁴⁷ Image edited from Rullière, C.; *Femtosecond Laser Pulses: Principles and Experiments*, Springer, 2005, p. 183
- ⁴⁸ Rullière, C.; *Femtosecond Laser Pulses: Principles and Experiments*, Springer, 2005, p. 183
- ⁴⁹ Image edited from <http://psj.nsu.ru/lector/lotov/terawatt/cpa.gif>
- ⁵⁰ Rullière, C.; *Femtosecond Laser Pulses: Principles and Experiments*, Springer, 2005, p. 184
- ⁵¹ Rullière, C.; *Femtosecond Laser Pulses: Principles and Experiments*, Springer, 2005, p. 202
- ⁵² http://www.physics.gatech.edu/gcuo/images/others/AC_fig01.gif
- ⁵³ Images from <http://www.physics.gatech.edu/gcuo/Tutorial/Autocorrelation.html>
- ⁵⁴ http://www.physics.gatech.edu/gcuo/images/others/FROG_fig01.gif
- ⁵⁵ Rullière, C.; *Femtosecond Laser Pulses: Principles and Experiments*, Springer, 2005, p. 217
- ⁵⁶ http://www.physics.gatech.edu/gcuo/images/others/FROG_fig05.gif
- ⁵⁷ <http://www.physics.gatech.edu/gcuo/lectures/UFO12UltrafastInterferometry.ppt>
- ⁵⁸ <http://ultrafast.physics.ox.ac.uk/spider/figures/figure5.gif>
- ⁵⁹ <http://ultrafast.physics.ox.ac.uk/spider/res.html>
- ⁶⁰ Keller, U.; *Recent Developments In Compact Ultrafast Lasers*, Nature, 424, 2003, p. 831
- ⁶¹ Zewail, A.H.; *Femtochemistry: Recent progress in studies of dynamics and control of reactions and their transition states*, J. Phys. Chem. 100, 1996, p. 12701
- ⁶² Zewail, A.H.; *Femtochemistry: atomic-scale dynamics of chemical bond*, J. Phys. Chem. A104, 2000, p. 5660–5694
- ⁶³ Ramaswami, R.; Sivarajan, K.; *Optical Networks: A Practical Perspective*, Morgan Kaufmann, 1998
- ⁶⁴ Mollenauer, L.F.; *et al.*; *Demonstration of massive wavelength-division multiplexing over transoceanic distances by use of dispersion-managed solitons*, Opt. Lett. 25, 2000, p. 704–706
- ⁶⁵ Miller, D.A.B.; *Optical interconnects to silicon*, IEEE J. Sel. Top. Quantum Electron. 6, 2000, p. 1312–1317
- ⁶⁶ Krishnamoorthy, A.V.; Miller, D.A.B.; *Scaling optoelectronic-VLSI circuits into the 21st century: a technology roadmap*, IEEE J. Sel. Top. Quantum Electron. 2, 1996, p. 55–76
- ⁶⁷ Zeller, S.C.; *et al.*; *Passively modelocked 40-GHz Er:Yb:glass laser*, Appl. Phys. B76, 2003, p. 787–788
- ⁶⁸ Huang, D.; *et al.*; *Optical coherence tomography*, Science 254, 1991, p. 1178–1181
- ⁶⁹ Holzwarth, R.; *et al.*; *Optical frequency synthesizer for precision spectroscopy*, Phys. Rev. Lett. 85, 2000, p. 2264–2267
- ⁷⁰ Holzwarth, R.; Zimmermann, M.; Udem, T.; Hänsch, T.W.; *Optical clockworks and the measurement of laser frequencies with a mode-locked frequency comb*, IEEE J. Quantum Electron. 37, 2001, p. 1493–1501
-

⁷¹ Udem, T.; Holzwarth, R.; Hänsch, T.W.; *Optical frequency metrology*, Nature 416, 2002, p. 233–237

⁷² Liu, X.; Du, D.; Mourou, G.; *Laser ablation and micromachining with ultrashort laser pulses*, IEEE J Quantum Electron. 33, 1997, p. 1706–1716

⁷³ Nolte, S.; et al.; *Ablation of metals by ultrashort laser pulses*, J. Opt. Soc. Am. B14, 1997, p. 2716–2722

⁷⁴ Juhasz, T.; Kurtz, R.; Horvath, C.; Suarez, C.; Raksi, F.; Spooner, G.; *The Femtosecond Blade: Applications in Corneal Surgery*, Optics & Photonics News, Jan 2002, p. 24-29

⁷⁵ Hammer, D.X.; et al.; *Experimental investigation of ultrashort pulse laser induced breakdown thresholds in aqueous media*, IEEE J. Quantum Electron. 32, 1996, p. 670–678

⁷⁶ Loesel, F.H.; Niemz, M.H.; Bille, J.F.; Juhasz, T.; *Laser-induced optical breakdown on hard and soft tissues and its dependence on the pulse duration: experiment and model*, IEEE J. Quantum Electron. 32, 1996, p. 1717–1722

⁷⁷ Personal communication from Dr. Rüdiger Paschotta, 24th March 2006

⁷⁸ http://www.rp-photonics.com/fiber_lasers_vs_bulk_lasers.html

⁷⁹ Krausz, F.; *Attosecond Spectroscopy Comes Of Age*, Optics & Photonics News, May 2002, p. 4